Supporting Information

Water splitting into hydrogen and oxygen by non-traditional redox inactive zinc selenolate electrocatalyst

Aditya Upadhyay, Saurav K. V., Manish Kumar, Evellin Lilly Varghese, Ananda S. Hodage, Amit Paul, Varadharajan Srinivasan and Sangit Kumar*

Department of Chemistry, Indian Institute of Science Education and Research (IISER) Bhopal-462 066 (India)

Supplementary Notes

Experimental Design: All reactions were carried out in oven-dried glassware with magnetic stirring. Zinc chloride used in this study were obtained from commercial sources and used without further purification. Solvent ethanol, propylene carbonate used here were obtained from commercial sources. Starting materials ortho-aminodiselenide and diselenide schiff base **2** were prepared by following literature procedure. NMR experiments were carried out on Bruker 400/500MHz spectrometer in CDCl3/DMSO-*d6* solvents and chemical shifts are reported in ppm. The following abbreviations were used to indicate multiplicity: s (singlet), d (doublet), t (triplet), q (quartet), dd (doublet of doublet), td (triplet of doublet) and m (multiplet). Electron paramagnetic resonance was carried out on Bruker EMX micro-X CW-EPR (34 GHz) series spectrophotometer. High resolution mass spectroscopic (HRMS) analysis is performed on quadrupole-time-of-flight Bruker MicroTOF-Q II mass spectrometer equipped with an ESI and APCI source; GC-MS analysis is performed on Agilent 7200/Agilent Technologies MS-S975C inert XLEI/CIMSD with triple axis detector. TLC plates (Merck silica gel (60F254) plates) used for monitoring the reactions were purchased from Merck. Single crystal X-ray data for compound **1** were collected on a Bruker D8 VENTURE diffractometer equipped with CMOS Photon 100 detector and Mo-Kα (λ = 0.71073 Å) radiation was used.

Electrochemistry: The electrochemical potential was converted relative to the normal hydrogen electrode (NHE; all potentials reported in this work are referenced to the NHE) following a literature protocol.[1]

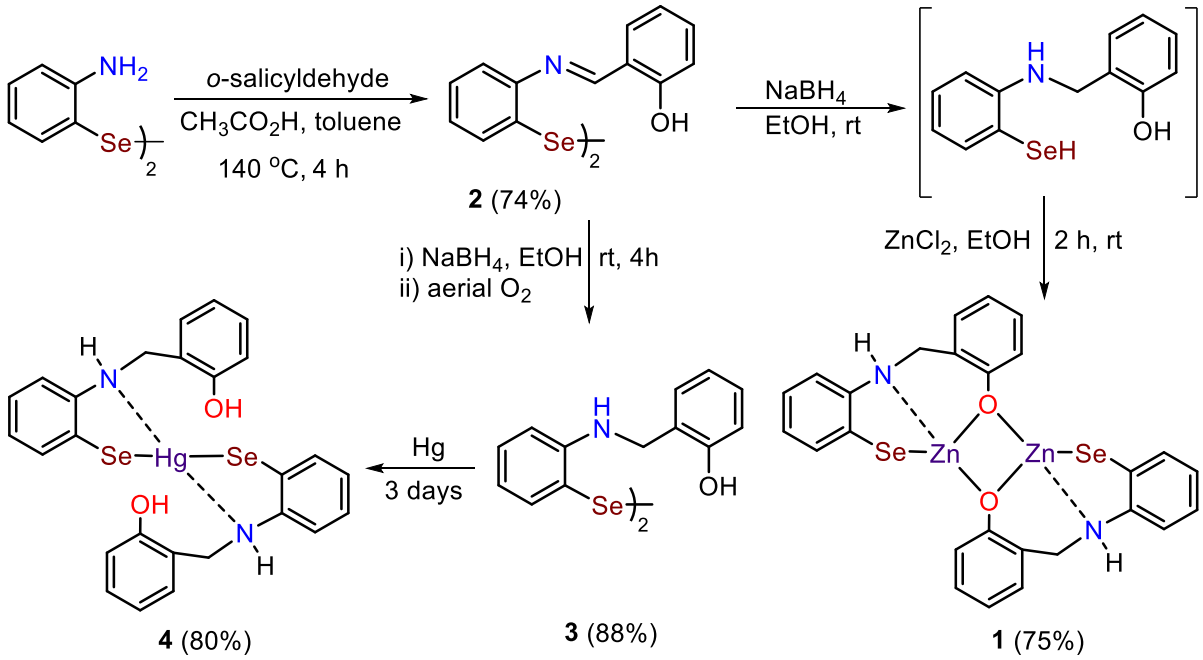

Scheme S1. Synthesis of Zinc and Mercuric selenolates

Precursor Schiff base and its reduced diselenide **2**[3] and **3**[3] are known amd were synthesized by copper-catalyzed method in gram quantity.[2]

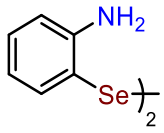

Bis (2-aminophenyl) diselenide:[2] To a DMF solution (8 mL), CuI (173 mg, 0.9 mmol, 0.2 equiv) and 1,10-phenanthroline (L) (164 mg, 0.9 mmol, 0.2 equiv) was added sequentially under nitrogen atmosphere and stirred for 15 min. at room temperature. To an orange colored solution of CuL, succinimide (450 mg, 4. 6 mmol, 1 equiv), 2-iodoaniline (1000 mg, 4.6 mmol, 1 equiv), Se powder (720 mg, 9.1 mmol, 2 equiv) and K_2CO_3 (945 mg, 6.8 mmol, 1.5 equiv) was added in a same order and stirred the reaction for 16 h at 140 °C. After this, the reaction mixture was poured into brine solution (80 mL) and stirred for 2 h at room temperature in air. Reaction mixture extracted by ethyl acetate (25 mL x 3). Combined organic layer was washed

with water (50 mL), dried over Na_2SO_4 and evaporated on rotatory evaporator under vacuo, which results in crystalline orange solid. Yield 1.09 g (70%).

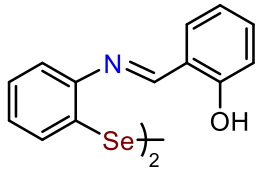

Schiff base 2:[3] In an oven dried round bottom flask, salicylaldehyde (160 µL, 1.5 mmol, 3 equiv) and acetic acid (8-10 drops) were added in 15 mL of toluene. After that, bis(2-aminophenyl)diselenide (172 mg, 0.5 mmol, 1 equiv) was added. The flask was fitted with water condenser and connected to Dean Stark apparatus, and the reaction mixture was allowed to stirred at 140 ^oC for 4 h. After the fully consumption of diselenide, the reaction mixture was cooled to room temperature and the solvent was removed on rotatory evaporator. The obtained crude solid was washed by hexane several times to afford yellow crystalline pure Schiff base. Yield 203 mg (74%)

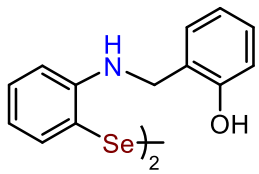

Reduced Schiff Base 3.[3] To an ethanolic solution of Schiff base **2** (138 mg, 0.25 mmol, 1 equiv), sodium borohydride (38 mg, 1 mmol, 4 equiv) was added at room temperature and stirred for 4 h at room temperature. After that, the reaction mixture was poured into aqueous sodium carbonate solution and the resulted solution stirred for 2 h at room temperature followed by extraction with ethyl acetate (25 mL x 3). The extracted reaction mixture was washed with brine and dried over Na_2SO_4 and the solvent was removed under vaccuo to yield crystalline yellow colored solid. Yield 122 mg (88%)

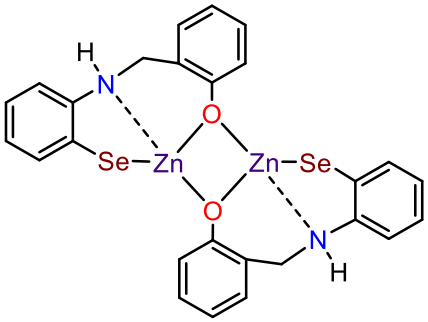

Bimetallic zinc selenolate complex 1: To the stirred solution of schiff base diselenide **2** (248 mg, 0.45 mmol, 1 equiv.) in ehtanol, we added sodium borohydride (76 mg, 2.0 mmol, 4 equiv) to generated in-situ selenol and stirred the solution upto 4 h at room tempreature**.** Then we added zinc chloride (122 mg, 0.9 mmol, 2 equiv.) and stirred the solution for 2 h. After that, the solvent was removed by rotatory evaporator and the solid residue was washed with aqueous sodium bicarbonate solution several times to afford a light yellow colored novel bimetallic zinc selenolate complex **1** in (230 mg) 75% yield. Crystallization was done in DMSO water (2:1) mixture to afford yellow colored crystals. ^{1}H NMR (400 MHz, DMSO-d_6) δ 9.63 (s, 1H) , 7.29 (d, J = 7.3 Hz, 1H) , 7.12 (d, J = 7.3 Hz, 1H) , 6.98 (t, J = 7.5 Hz, 1H) , 6.83 (m, J = 7.4 Hz, 2H) , 6.63 (t, J = 7.4 Hz, 1H) , 6.35 (d, J = 8.0 Hz, 1H) , 6.22 (t, J = 7.3 Hz, 1H) , 5.42 (s, J = 6.2 Hz, 1H), 4.22 (s, 1H);^{13}C NMR (101 MHz, DMSO-d_6) δ 168.34, 146.17, 136.39, 135.38, 131.39, 129.55, 126.07, 124.76, 124.27, 123.77, 119.88, 112.62, 55.73. ^{77}Se NMR (76 MHz, DMSO-d_6) δ -84.73. HRMS of $[M + nH]^{+}$= 682.8659, found 682.8652.

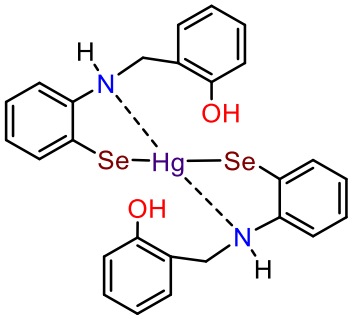

Monometallic mercuric selenolate complex 4: Next, the standard elemental mercury (108 mg, 0.54 mmol, 1 equiv.) was added to the stirred ethanolic solution of reduced diselendie **3** (300 mg, 0.54 mmol, 1 equiv.) at room tempreature for 3 days which results in the insertion of Hg into Se─Se bond of reduced diselenide **3**. Then the reaction mixture was filtered over celite, and solvent was removed under rotatory evaporator to afforded a green colored monometallic mercury selenolate complex **4**. Yield 327 mg (80%). ^{1}H NMR (400 MHz, DMSO-d_6) δ 7.29 (d, *J* = 7.3 Hz, 1H), 7.12 (d, *J* = 7.3 Hz, 1H), 6.98 (t, *J* = 7.5 Hz, 1H), 6.83 (q, *J* = 7.3 Hz, 2H), 6.63 (t, *J* = 7.4 Hz, 1H), 6.35 (d, *J* = 8.0 Hz, 1H), 6.22 (t, *J* = 7.3 Hz, 1H), 4.22 (d, *J* = 5.1 Hz, 2H); ^{13}C NMR (101 MHz, DMSO-d_6) δ 155.38, 148.99, 137.28, 128.69, 128.25, 127.93, 125.79, 119.33, 116.68, 115.26, 114.42, 110.44, 42.49; ^{77}Se NMR (76 MHz, DMSO-d_6) δ 75.70. HRMS of [M+nH]= 758.9956, found 758.9977

^{1}H NMR of **1**

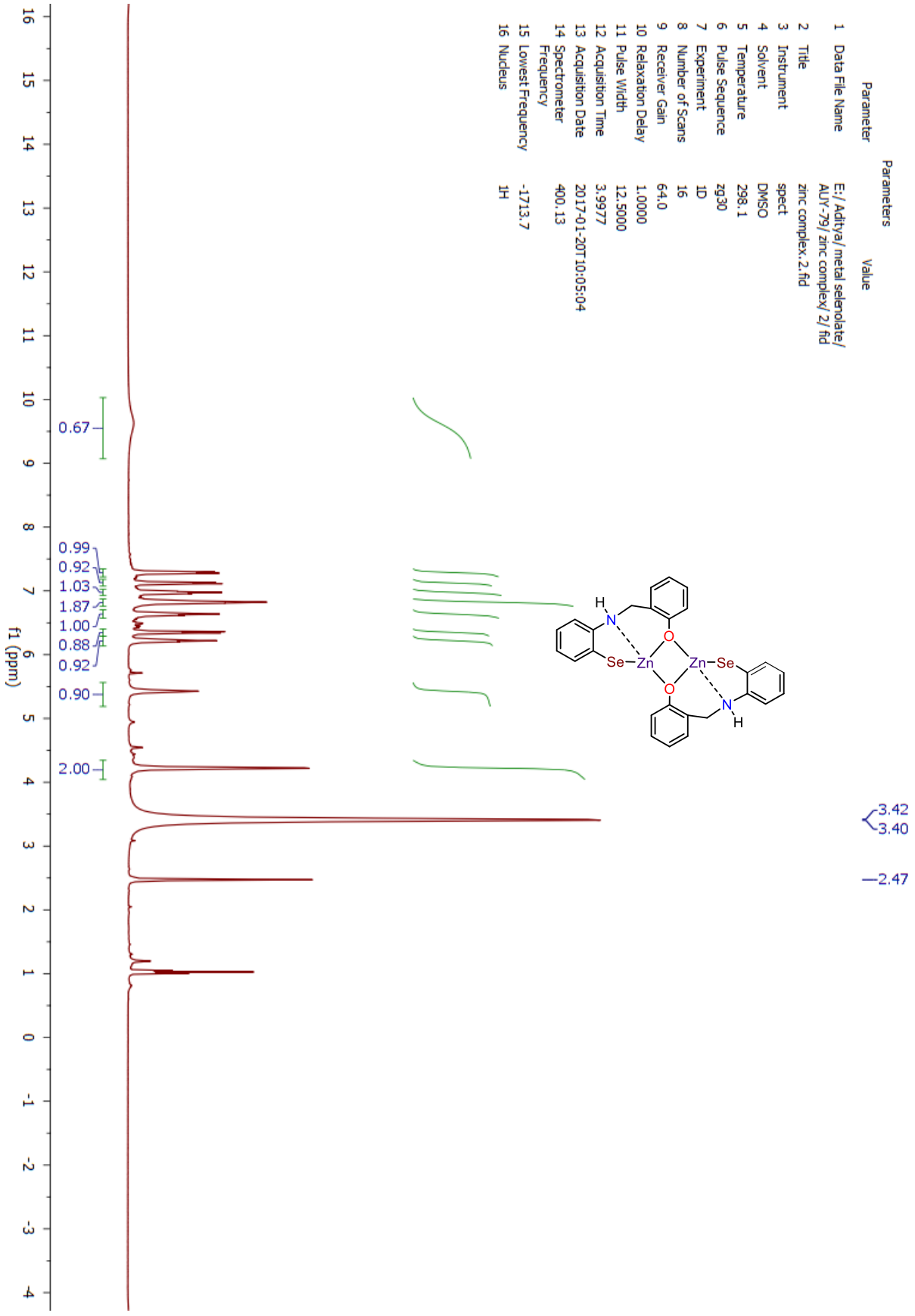
Parameters
Parameter
Value
1 Data File Name E:/ Aditya/ metal selenolate/ AUY-79/ zinc complex/ 2/ fid
2 Title zinc complex.2.fid
3 Instrument spect
4 Solvent DMSO
5 Temperature 298.1
6 Pulse Sequence zg30
7 Experiment 1D
8 Number of Scans 16
9 Receiver Gain 64.0
10 Relaxation Delay 1.0000
11 Pulse Width 12.5000
12 Acquisition Time 3.9977
13 Acquisition Date 2017-01-20T10:05:04
14 Spectrometer Frequency 400.13
15 Lowest Frequency -1713.7
16 Nucleus 1H
0.67
0.99
0.92
1.03
1.87
1.00
0.88
0.92
0.90
2.00
3.42
3.40
2.47
f1 (ppm)
H
N
O
Se
Zn
Zn
Se
O
N
H

^{13}C NMR of **1**

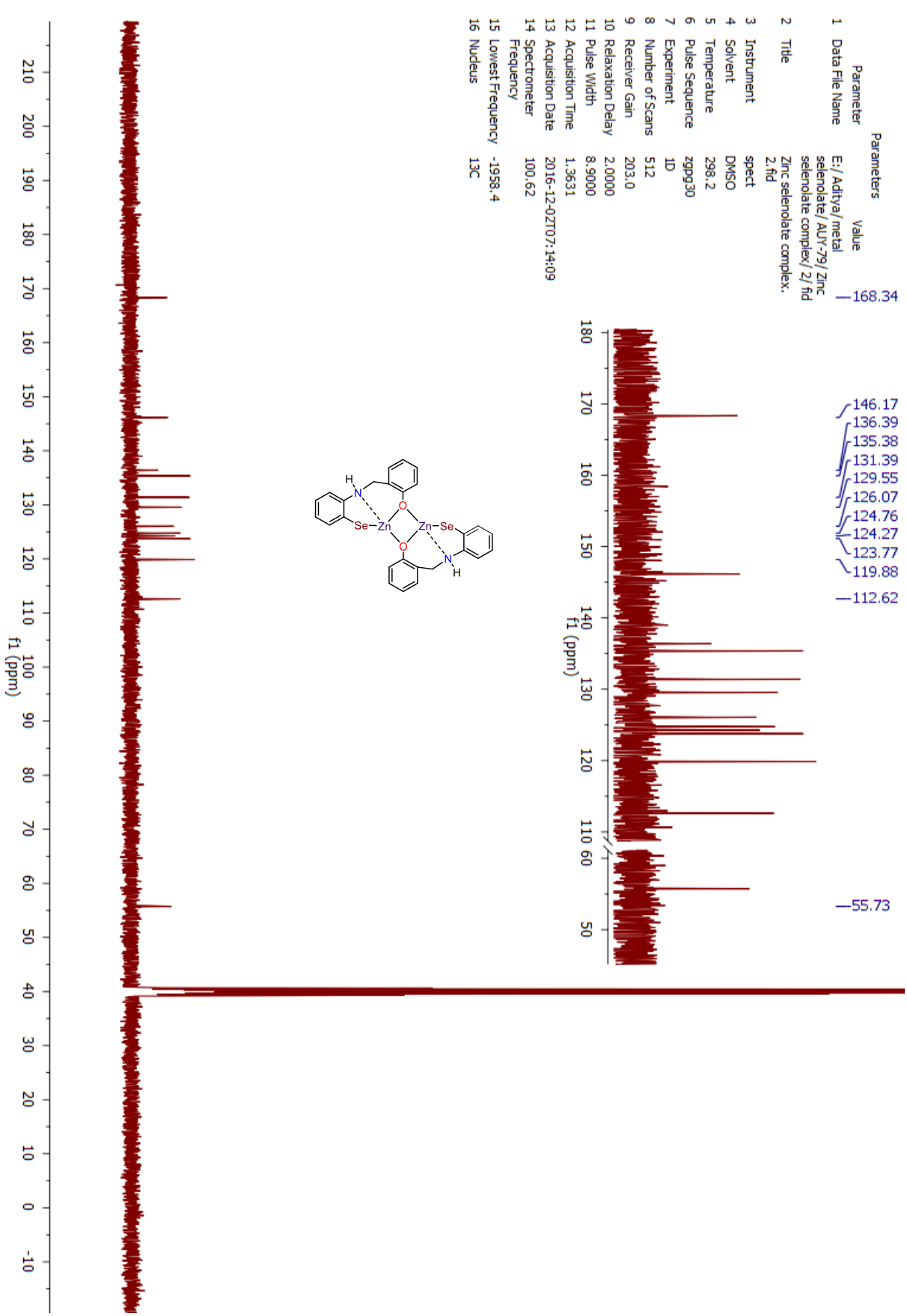
Parameters
Parameter Value
1 Data File Name E:/ Aditya/ metal selenolate/ AUY-79/ Zinc selenolate complex/ 2/ fid
2 Title Zinc selenolate complex. 2.fid
3 Instrument spect
4 Solvent DMSO
5 Temperature 298.2
6 Pulse Sequence zgpg30
7 Experiment 1D
8 Number of Scans 512
9 Receiver Gain 203.0
10 Relaxation Delay 2.0000
11 Pulse Width 8.9000
12 Acquisition Time 1.3631
13 Acquisition Date 2016-12-02T07:14:09
14 Spectrometer Frequency 100.62
15 Lowest Frequency -1958.4
16 Nucleus 13C
168.34
146.17
136.39
135.38
131.39
129.55
126.07
124.76
124.27
123.77
119.88
112.62
55.73
f1 (ppm)

^{77}Se NMR of **1**

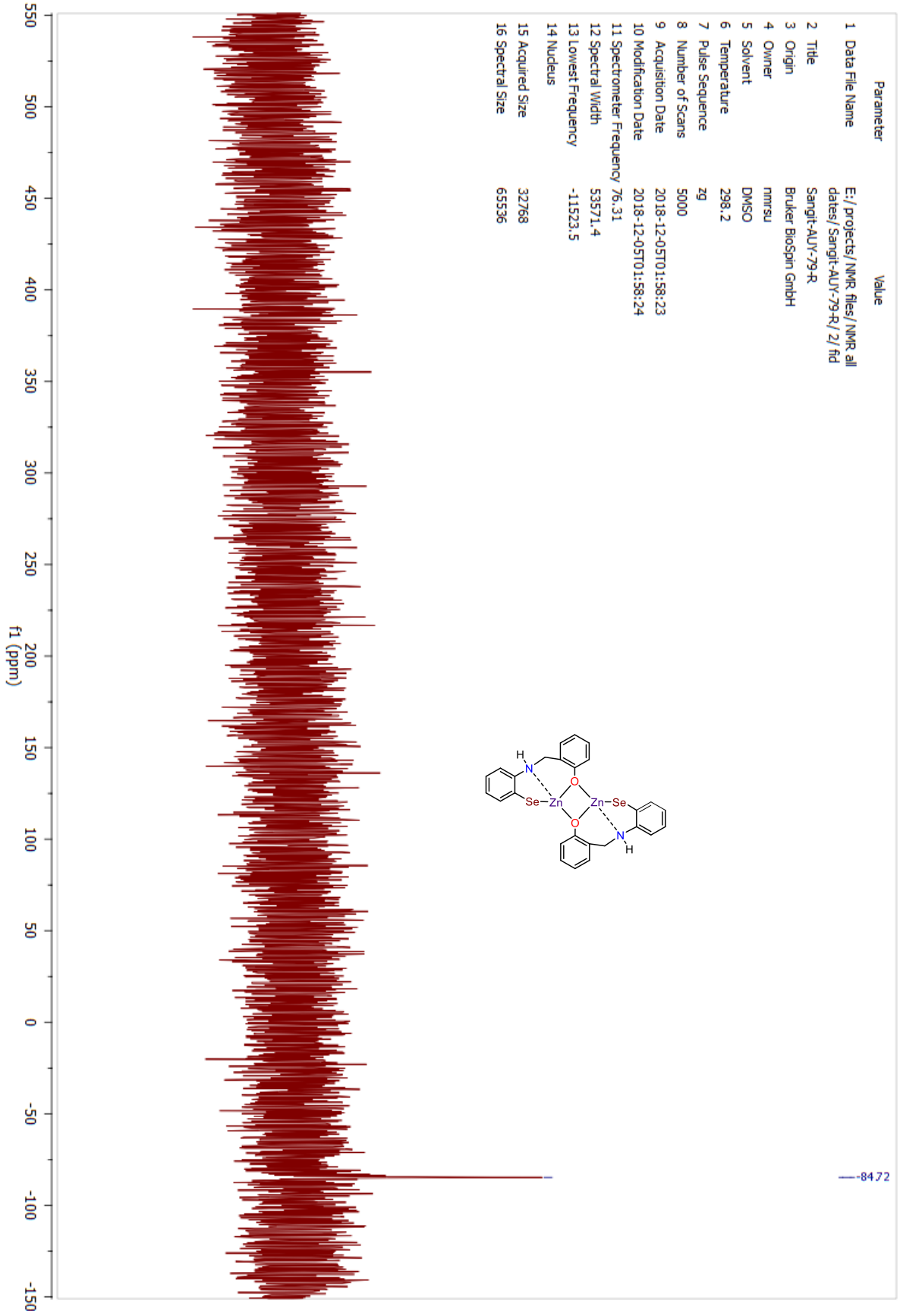
Parameter
Value
1 Data File Name
E:/ projects/ NMR files/ NMR all dates/ Sangit-AUY-79-R/ 2/ fid
2 Title
Sangit-AUY-79-R
3 Origin
Bruker BioSpin GmbH
4 Owner
nmrsu
5 Solvent
DMSO
6 Temperature
298.2
7 Pulse Sequence
zg
8 Number of Scans
5000
9 Acquisition Date
2018-12-05T01:58:23
10 Modification Date
2018-12-05T01:58:24
11 Spectrometer Frequency 76.31
12 Spectral Width
53571.4
13 Lowest Frequency
-11523.5
14 Nucleus
15 Acquired Size
32768
16 Spectral Size
65536
-84.72
f1 (ppm)
550
500
450
400
350
300
250
200
150
100
50
0
-50
-100
-150

HRMS data of **1**

Display Report

Analysis Info

Acquisition Date	12/20/2018 12:28:09 PM		
Analysis Name	D:\Data\NEW USER DATA 2017\2018\DECEMBER\19 DEC\Dr S Kumar-AUY-79-R.d		
Method	tune_low_APCI.m	Operator	RUCHI
Sample Name	AUY-79-R	Instrument	micrOTOF-Q II 10330
Comment			

Acquisition Parameter

Source Type	APCI	Ion Polarity	Positive	Set Nebulizer	2.5 Bar
Focus	Not active	Set Capillary	4500 V	Set Dry Heater	200 °C
Scan Begin	50 m/z	Set End Plate Offset	-500 V	Set Dry Gas	4.0 l/min
Scan End	3000 m/z	Set Collision Cell RF	300.0 Vpp	Set Divert Valve	Waste

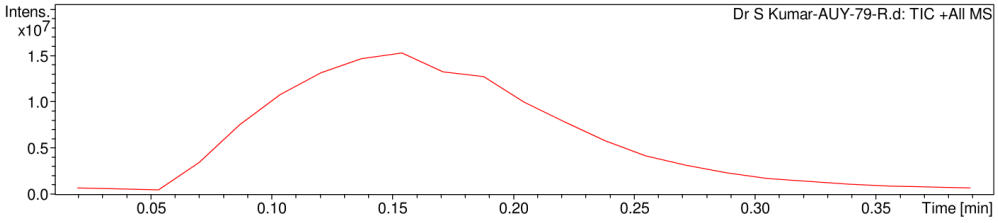

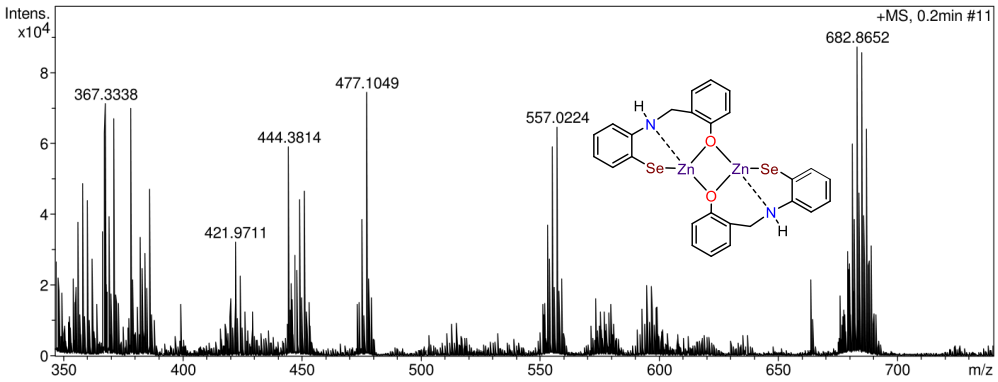

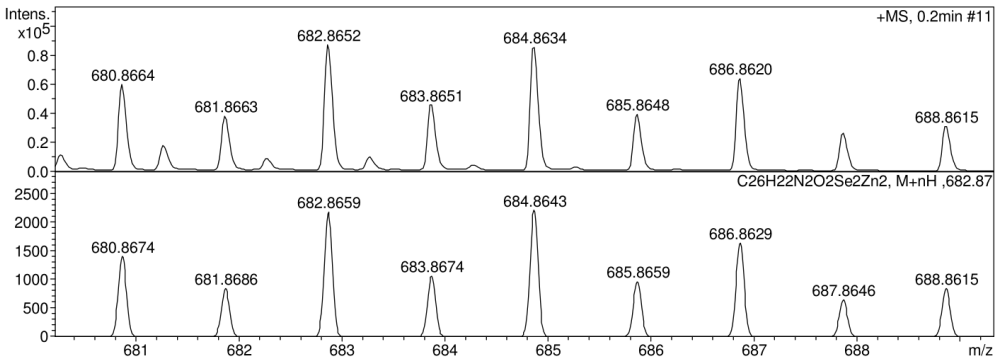

Bruker Compass DataAnalysis 4.0 printed: 12/20/2018 12:29:47 PM Page 1 of 1

1H NMR of **4**

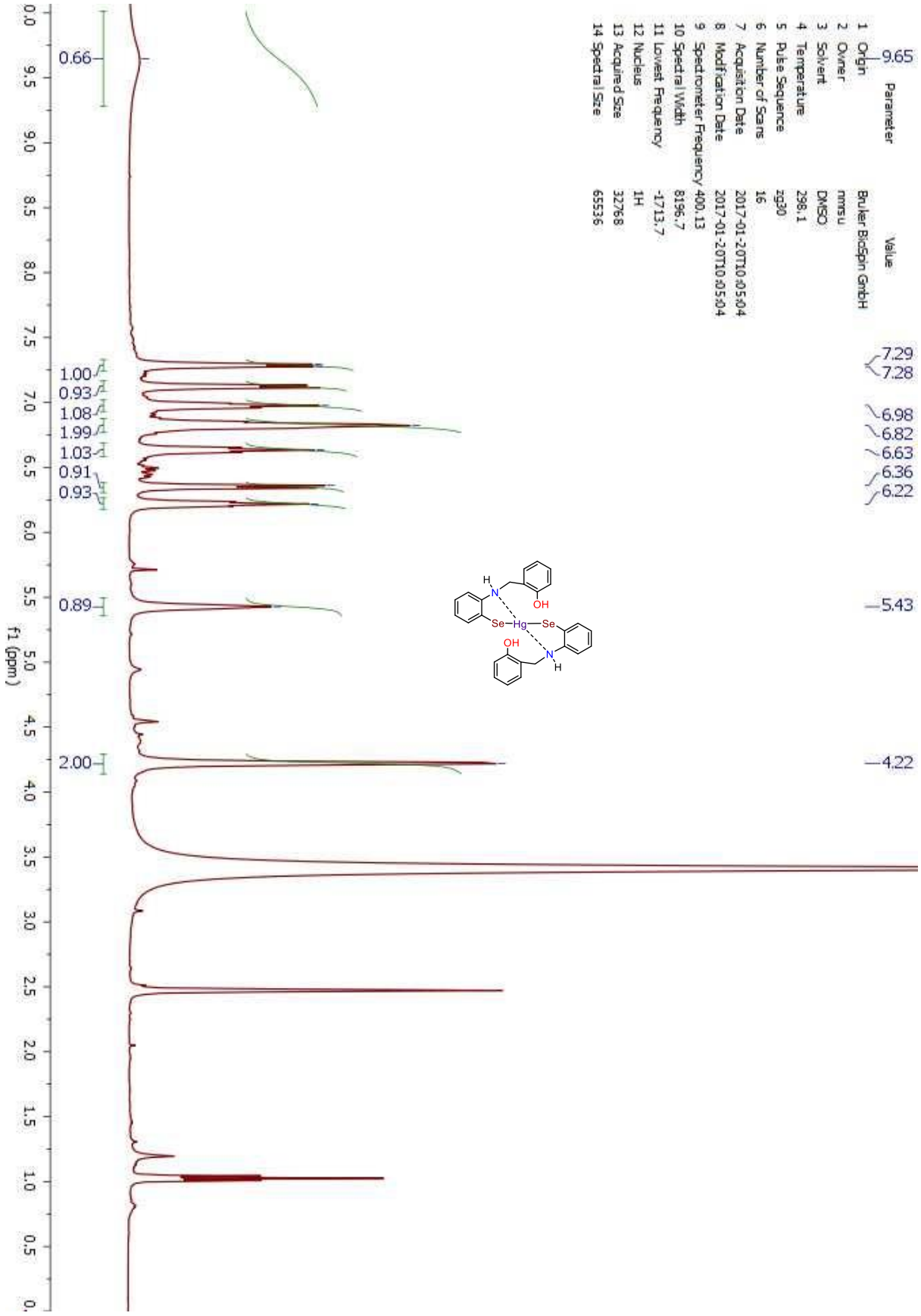
Parameter
Value
1 Origin
Bruker BioSpin GmbH
2 Owner
nmrsu
3 Solvent
DMSO
4 Temperature
298.1
5 Pulse Sequence
zg30
6 Number of Scans
16
7 Acquisition Date
2017-01-20T10:05:04
8 Modification Date
2017-01-20T10:05:04
9 Spectrometer Frequency 400.13
10 Spectral Width
8196.7
11 Lowest Frequency
-1713.7
12 Nucleus
1H
13 Acquired Size
32768
14 Spectral Size
65536
9.65
7.29
7.28
6.98
6.82
6.63
6.36
6.22
5.43
4.22
0.66
1.00
0.93
1.08
1.99
1.03
0.91
0.93
0.89
2.00
f1 (ppm)
H
N
OH
Se
Hg
Se
OH
N
H

^{13}C NMR of **4**

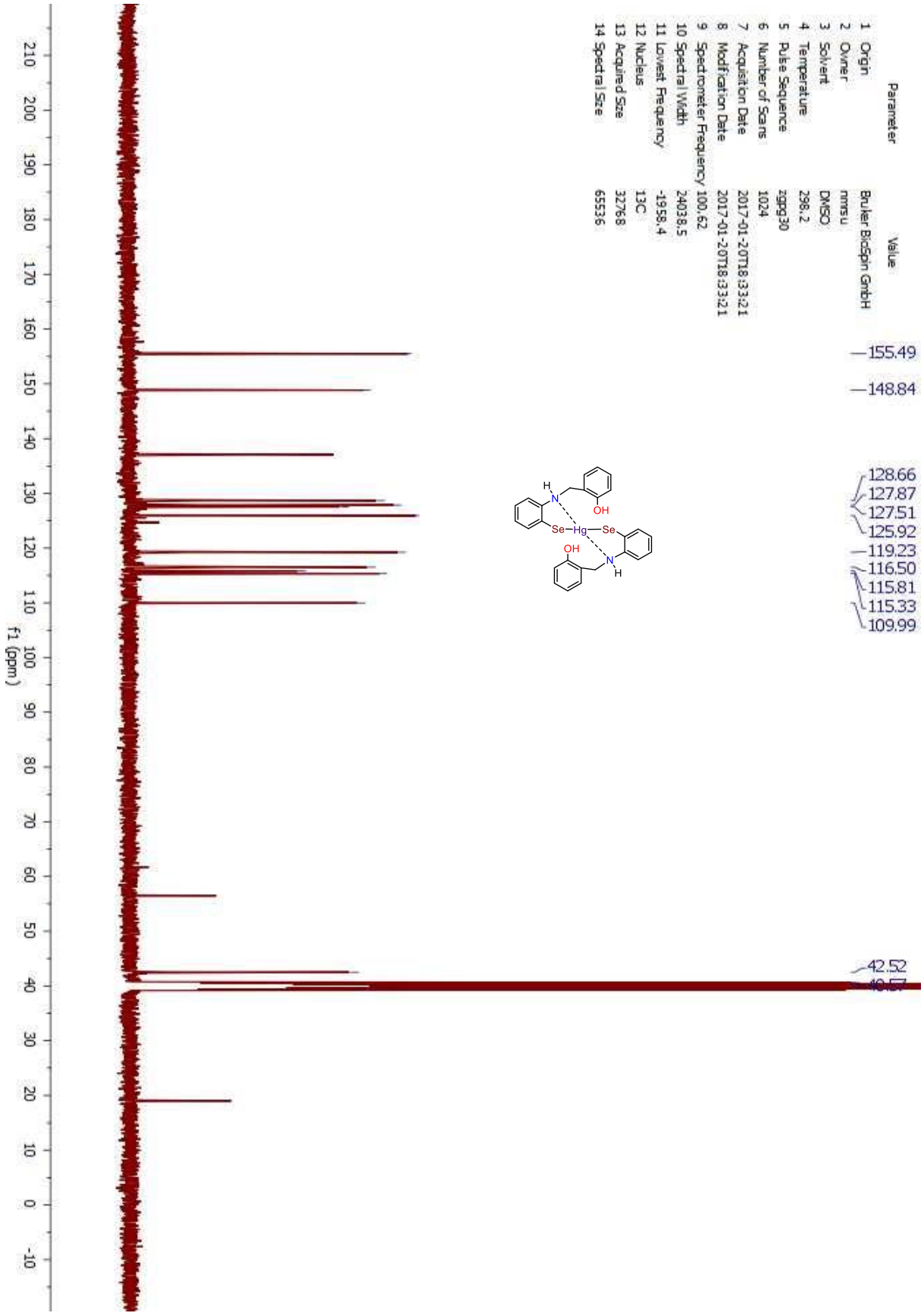
Parameter
Value
1 Origin
Bruker BioSpin GmbH
2 Owner
nmrsu
3 Solvent
DMSO
4 Temperature
298.2
5 Pulse Sequence
zgpg30
6 Number of Scans
1024
7 Acquisition Date
2017-01-20T18:33:21
8 Modification Date
2017-01-20T18:33:21
9 Spectrometer Frequency
100.62
10 Spectral Width
24038.5
11 Lowest Frequency
-1958.4
12 Nucleus
13C
13 Acquired Size
32768
14 Spectral Size
65536
155.49
148.84
128.66
127.87
127.51
125.92
119.23
116.50
115.81
115.33
109.99
42.52
H
N
OH
Se
Hg
Se
OH
N
H
f1 (ppm)

^{77}Se NMR of **4**

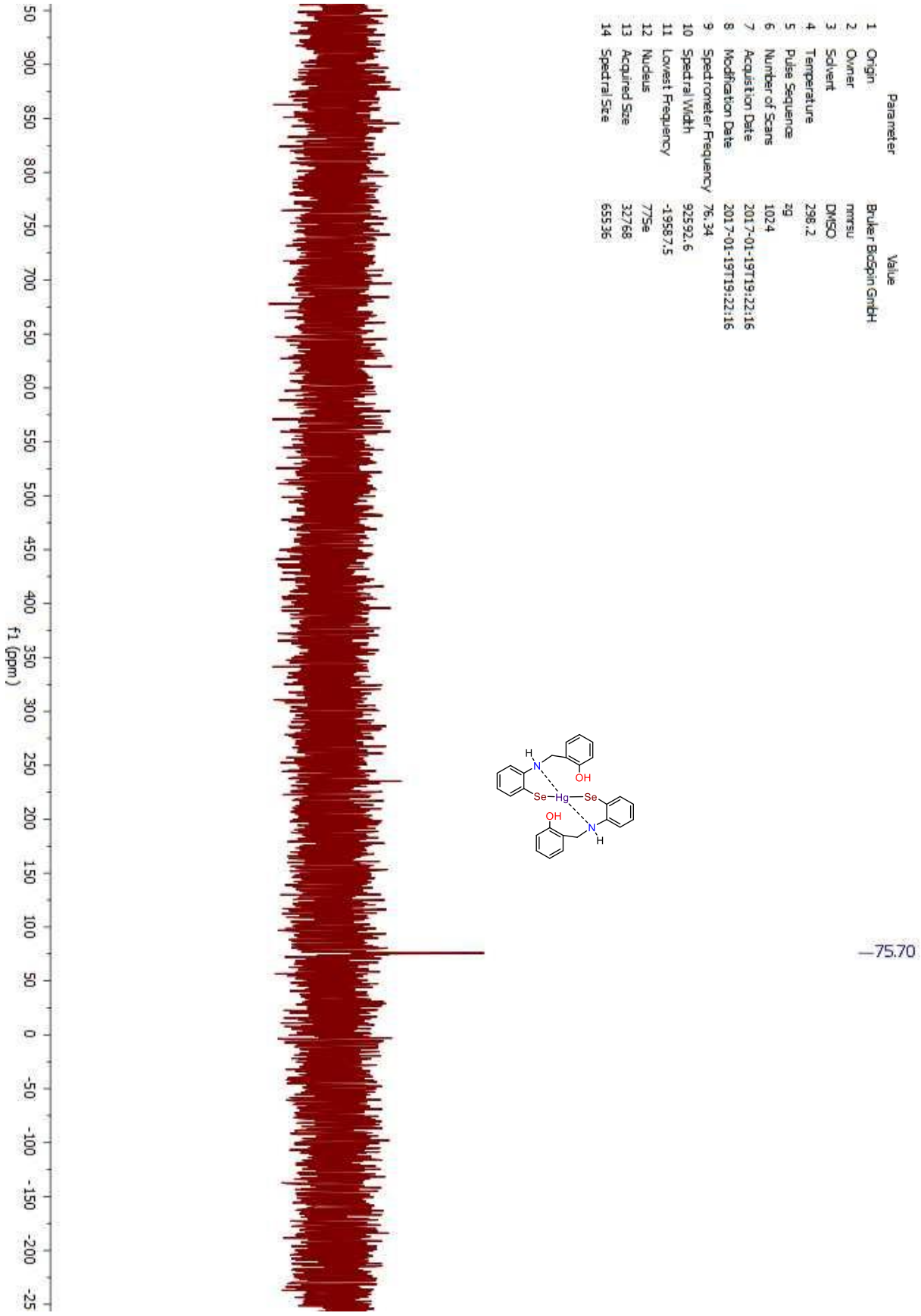
Parameter Value
1 Origin Bruker BioSpin GmbH
2 Owner nmrsu
3 Solvent DMSO
4 Temperature 298.2
5 Pulse Sequence zg
6 Number of Scans 1024
7 Acquisition Date 2017-01-19T19:22:16
8 Modification Date 2017-01-19T19:22:16
9 Spectrometer Frequency 76.34
10 Spectral Width 92592.6
11 Lowest Frequency -19587.5
12 Nucleus 77Se
13 Acquired Size 32768
14 Spectral Size 65536
H
N
OH
Se
Hg
Se
OH
N
H
75.70
f1 (ppm)
50 900 850 800 750 700 650 600 550 500 450 400 350 300 250 200 150 100 50 0 -50 -100 -150 -200 -25

HRMS data of **4**

Display Report

Analysis Info

Analysis Name	D:\Data\NEW USER DATA 2017\2019\JAN\10 jan\Prof.S.Kumar-AUY-75.d	Acquisition Date	1/10/2019 3:16:42 PM
Method	tune_wide _APCI_23.06.m	Operator	RUCHI
Sample Name	AUY-75	Instrument	micrOTOF-Q II 10330
Comment			

Acquisition Parameter

Source Type	APCI	Ion Polarity	Positive	Set Nebulizer	2.5 Bar
Focus	Not active	Set Capillary	4000 V	Set Dry Heater	200 °C
Scan Begin	50 m/z	Set End Plate Offset	-500 V	Set Dry Gas	4.0 l/min
Scan End	3000 m/z	Set Collision Cell RF	600.0 Vpp	Set Divert Valve	Waste

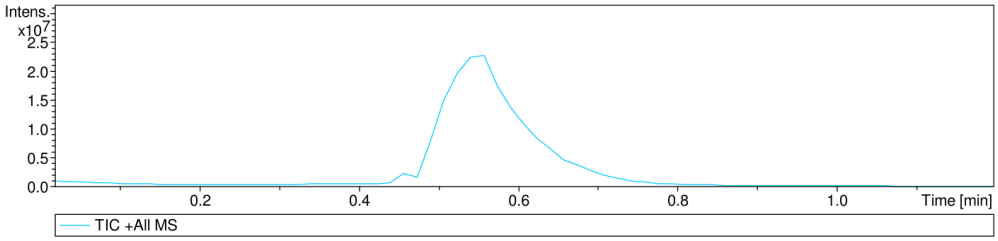

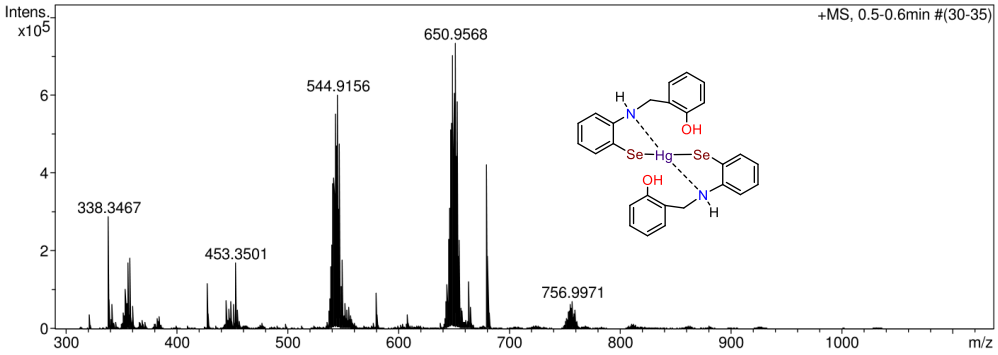

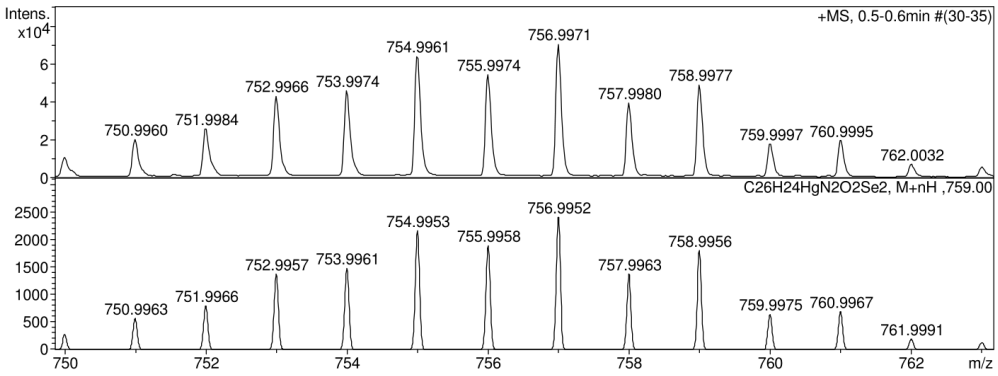

Crystal structure of bimetallic zinc selenolate complex 1 (CCDC No. 1949548)

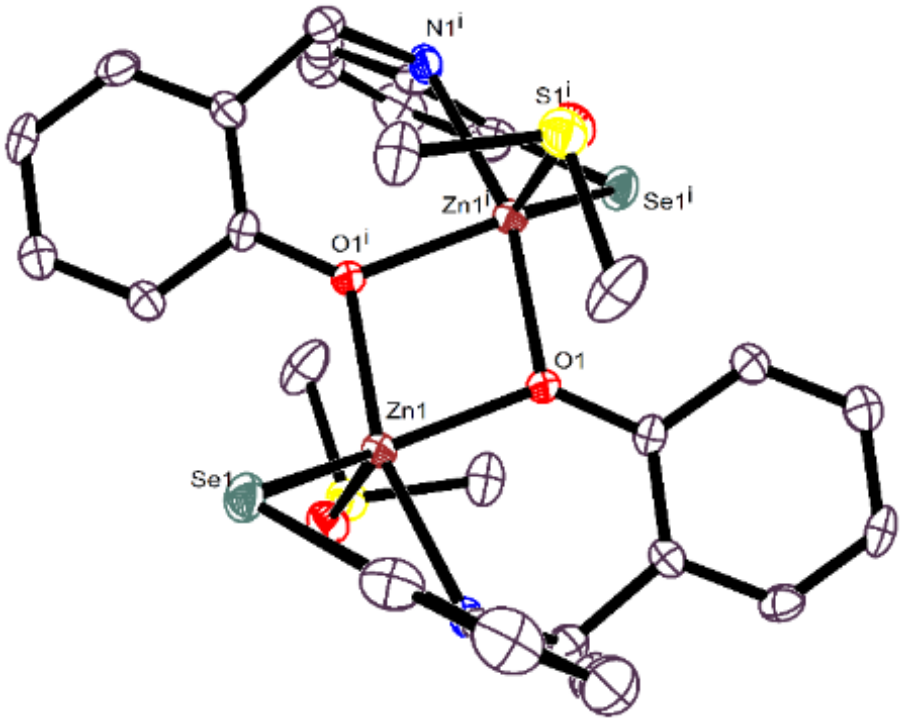

Packing diagram of bimetallic zinc selenolate complex 1

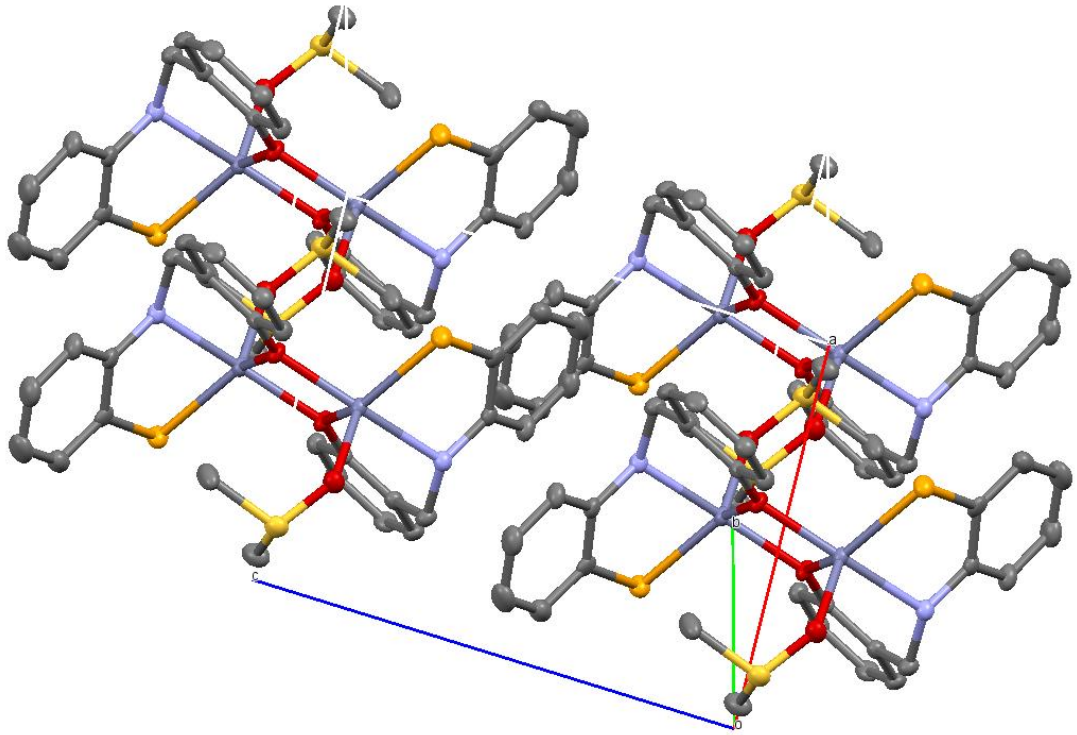

Table S1. Cystal data and structure refinement for 1

CCDC No.	1949548
Empirical formula	C15 H17 N O2 S Se Zn
Formula weight	420.69
Temperature	164(2) K
Wavelength	0.71073 Å
Crystal system	Triclinic
Space group	P -1
Unit cell dimensions	a = 8.4306(14) Å α= 76.941(6)°.
	b = 9.2108(16) Å β= 88.026(5)°.
	c = 10.5745(18) Å γ = 75.718(6)°.
Volume	775.0(2) $Å^3$
Z	2
Density (calculated)	1.803 Mg/m3
Absorption coefficient	4.070 mm-1
F(000)	422
Theta range for data collection	2.494 to 30.033°.
Index ranges	-11<=h<=11, -12<=k<=12, 0<=l<=14
Reflections collected	4284
Independent reflections	4284

Completeness to theta= 25.242°	99.9 %
Refinement method	Full-matrix least-squares on F2
Data / restraints / parameters	4284 / 0 / 196
Goodness-of-fit on F^2	0.882
Final R indices [I>2sigma(I)]	R1 = 0.0477, wR2 = 0.1104
R indices (all data)	R1 = 0.1034, wR2 = 0.1405
Extinction coefficient	n/a
Largest diff. peak and hole	0.818 and -0.665 e.Å-

Table S2. Selected Bond Length [Å] for **1**

Se1—C1	1.910 (4)	Zn1i—N1i	2.199 (3)
Se1—Zn1	2.4455 (7)	Zn1i—O1i	2.031 (3)
Zn1—O1	2.031 (3)	Se1i—Zn1i	2.4455 (7)
Zn1-N1	2.199(3)	Se1i—C1i	1.910 (4)
Zn1—O1i	2.058 (3)	Zn1i—O1	2.058 (3)

Table S2. Selected Bond Angle [º] for **1**

C1—Se1—Zn1	89.3 (1)	O1—Zn1i—O1i	78.2 (1)
Se1—Zn1—N1	82.2 (9)	Zn1i—O1i—Zn1	101.8 (1)
Zn1—N1—C6	108.7 (3)	C1i—Se1i—Zn1i	89.3 (1)
O1—Zn1—O1i	78.2(1)	Se1i—Zn1i—N1i	82.22 (9)
Zn1i—O1—Zn1	101.8 (1)	Zn1i—N1i—C6i	108.7 (3)

HRMS of intermediates 1a

An aliquot from the mixture of zinc selenolate **1** and hydrogen peroxide in the propylene carbonate/water solution were screened for mass spectrometry.

Calculated m/z = 719.8775

Experimental m/z = 719.3094

Isotopic Pattern = 715.3123, 716.3125, 717.3105, 718.3127, 719.3094, 720.3118, 721.3117, 722.3161

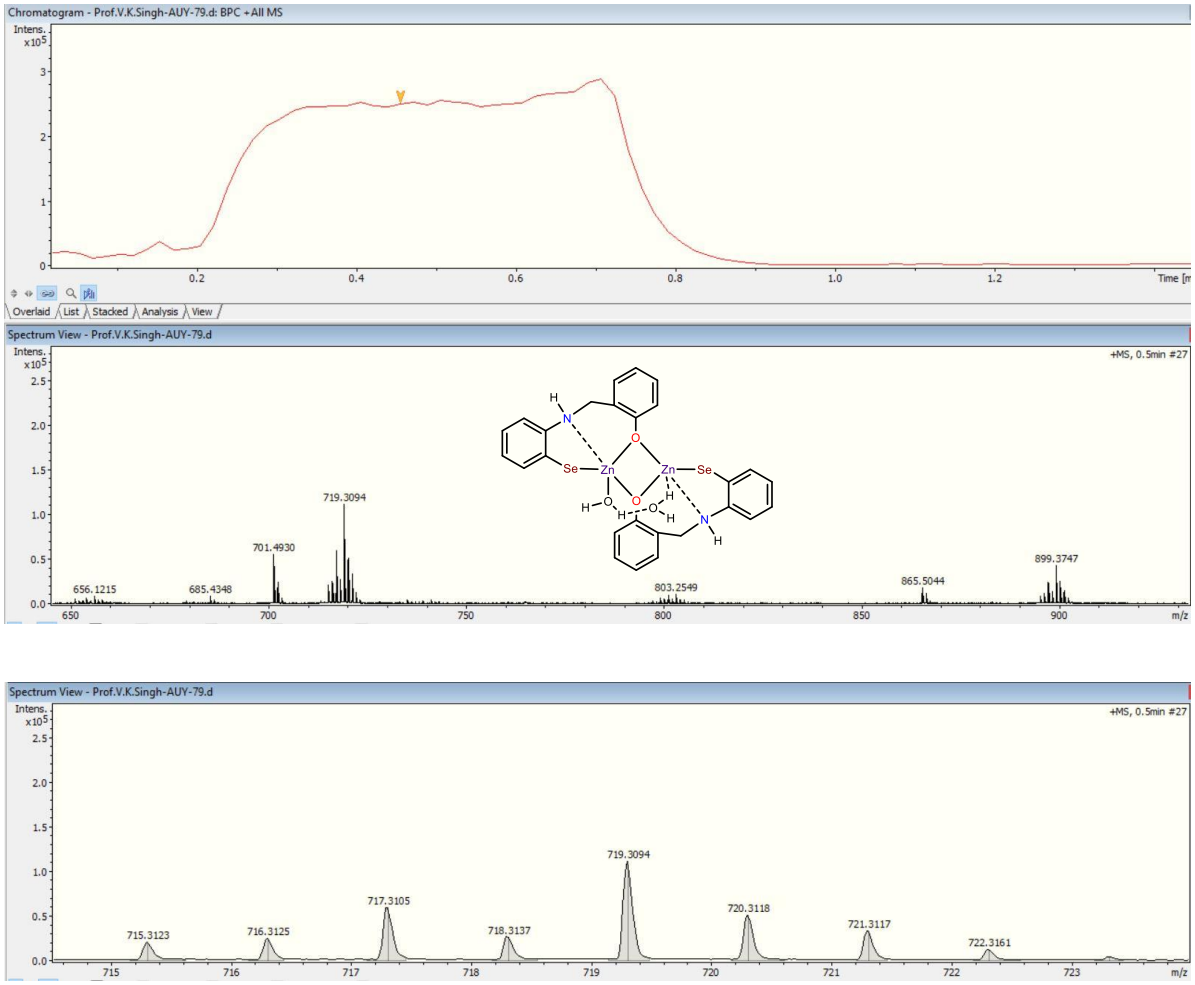

Figure S1. HRMS data of the reaction mixture of zinc selenolate **1** and hydrogen peroxide in the propylene carbonate/water solution for intermediate **1a**

HRMS of intermediates 1b

An aliquot from the mixture of zinc selenolate **1** and hydrogen peroxide in the propylene carbonate/ water solution were screened for mass spectrometry.

Calculated m/z = 718.1760

Experimental m/z = 718.1469

Isotopic Pattern = 714.1418, 715.1354, 716.1454, 717.1574, 718.1469, 719.1486, 720.1508, 721.1477, 722.1039

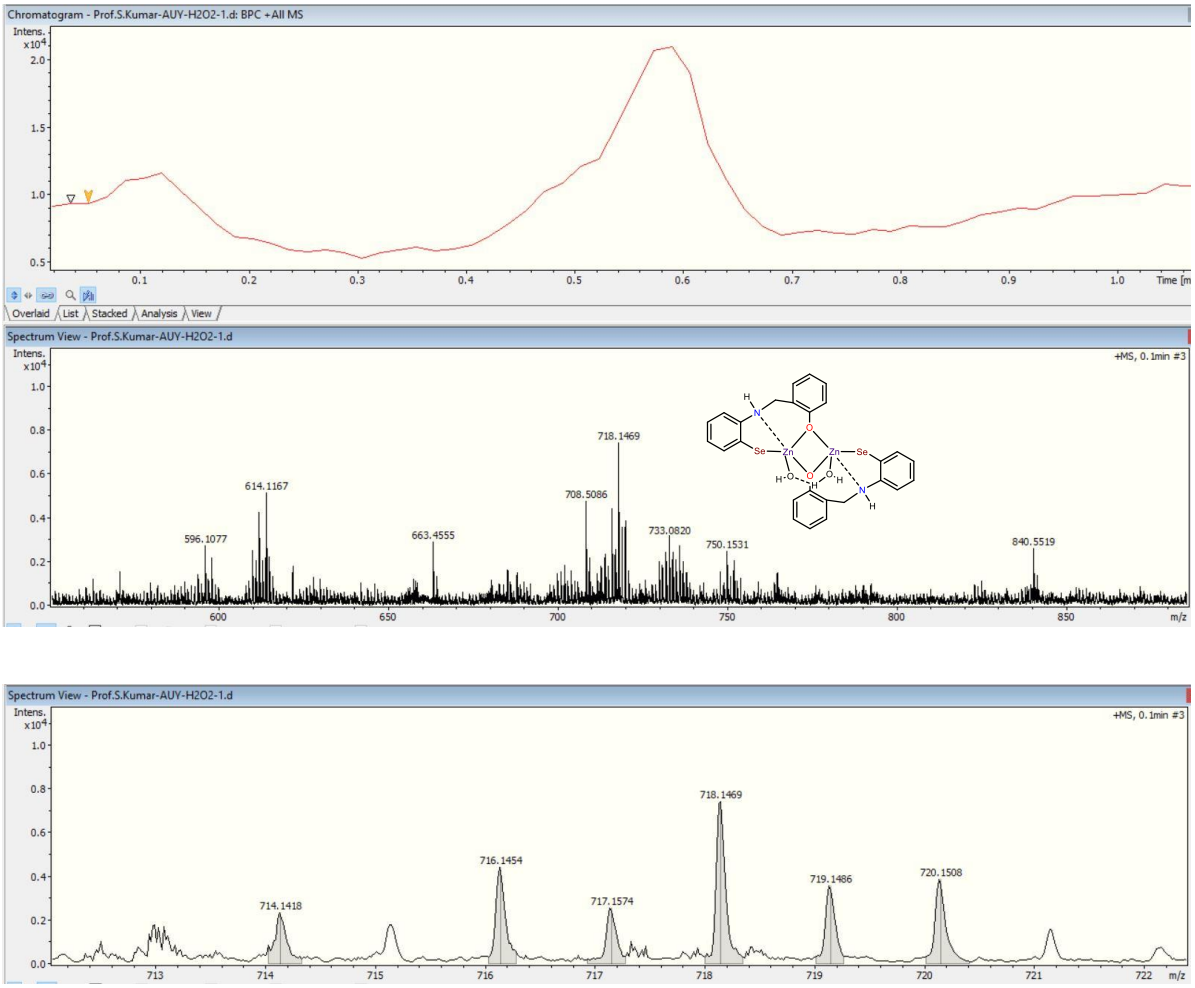

Figure S2. HRMS data of the reaction mixture of zinc selenolate **1** and hydrogen peroxide in the propylene carbonate/water solution for intermediate **1b**.

Electrochemical Studies

OER by zinc selenolate complex 1 with water

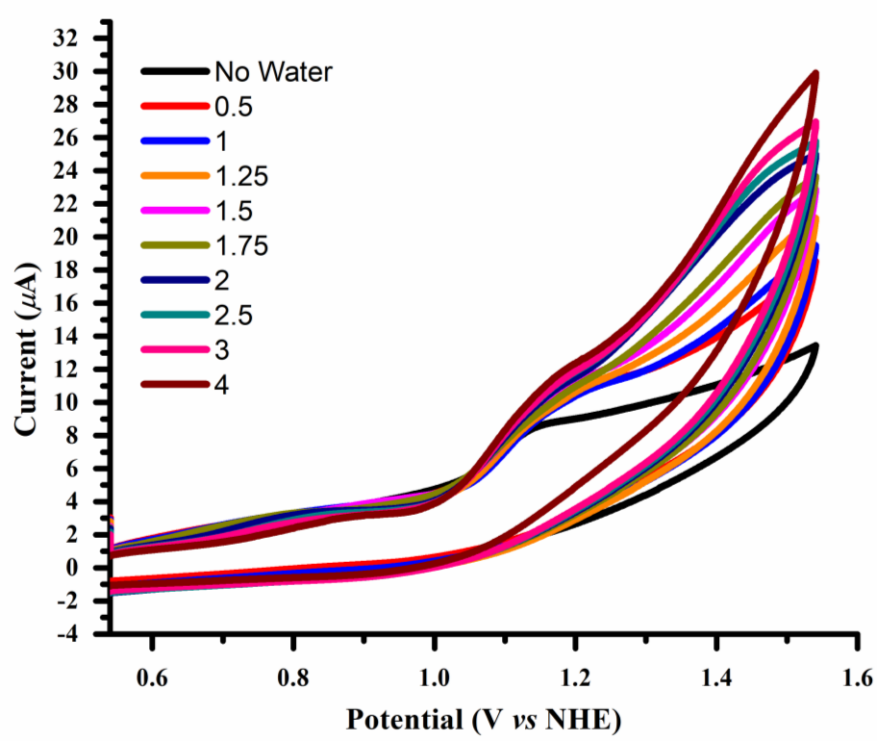

Figure S3. Cyclic Voltammogram of bimetallic zinc selenolate **1** (1mM) using 0.1M $^{n}Bu_4NPF_6$ as supporting electrolyte in propylene carbonate solution with varying the concentration of water up to 4% for oxygen evolution reaction (OER) from water.

i_{cat}/i_p *vs.* $[H_2O]^{1/2}$

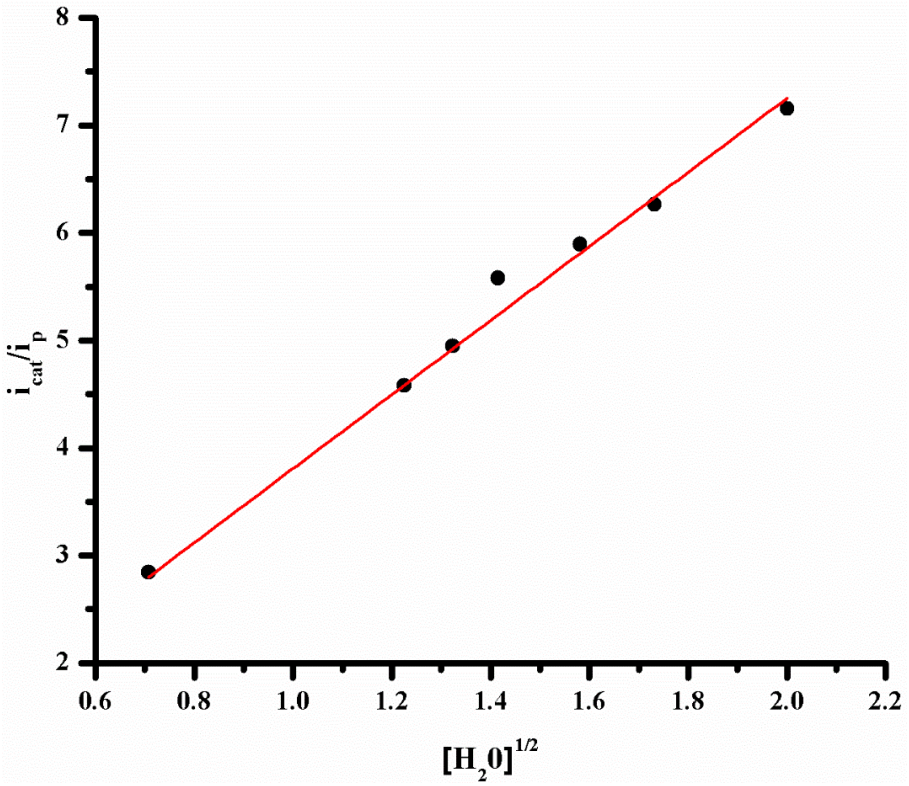

Figure S4. Corresponding linear plot (for OER) of i_{cat} *vs.* $[H_2O]^{1/2}$ with scan rate 20 mv/s.

%R- square = 97.857, slope = 3.445 ± 0.3

Electrocatalysis at different scan rates

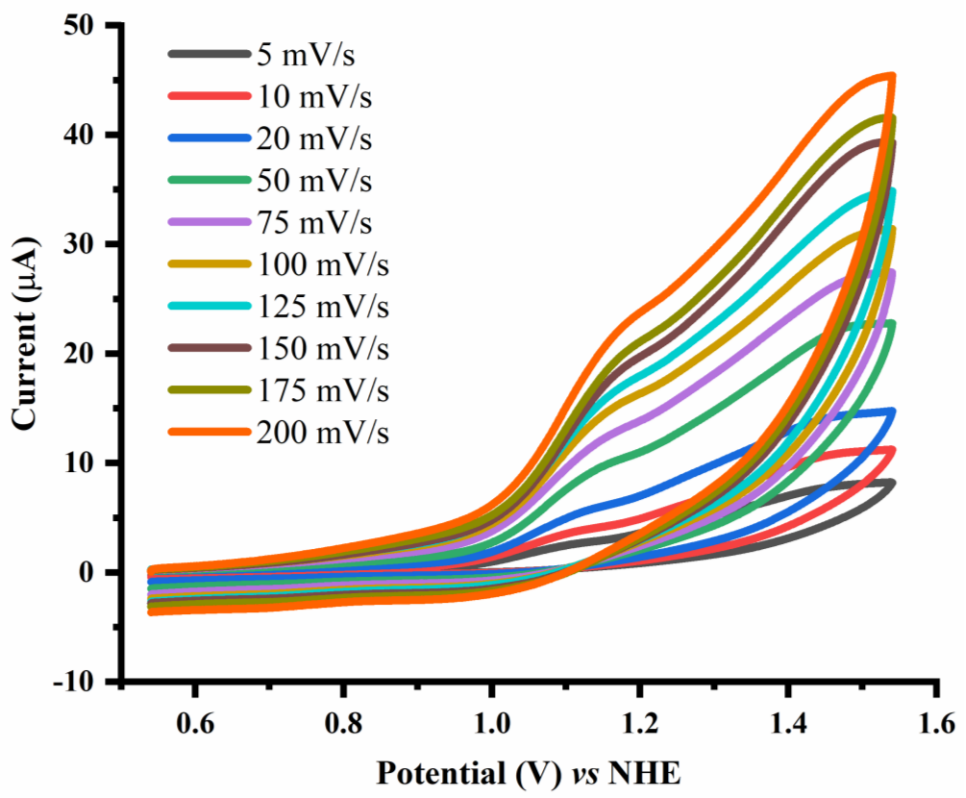

Figure S5. Cyclic Voltammogram of bimetallic zinc selenolate **1** (1mM) using 0.1M $^{n}Bu_4NPF_6$ as supporting electrolyte in propylene carbonate solution with varying the 1% of water at varying scan rates from 5 mV/s to 200 mV/s for oxygen evolution reaction (OER) from water

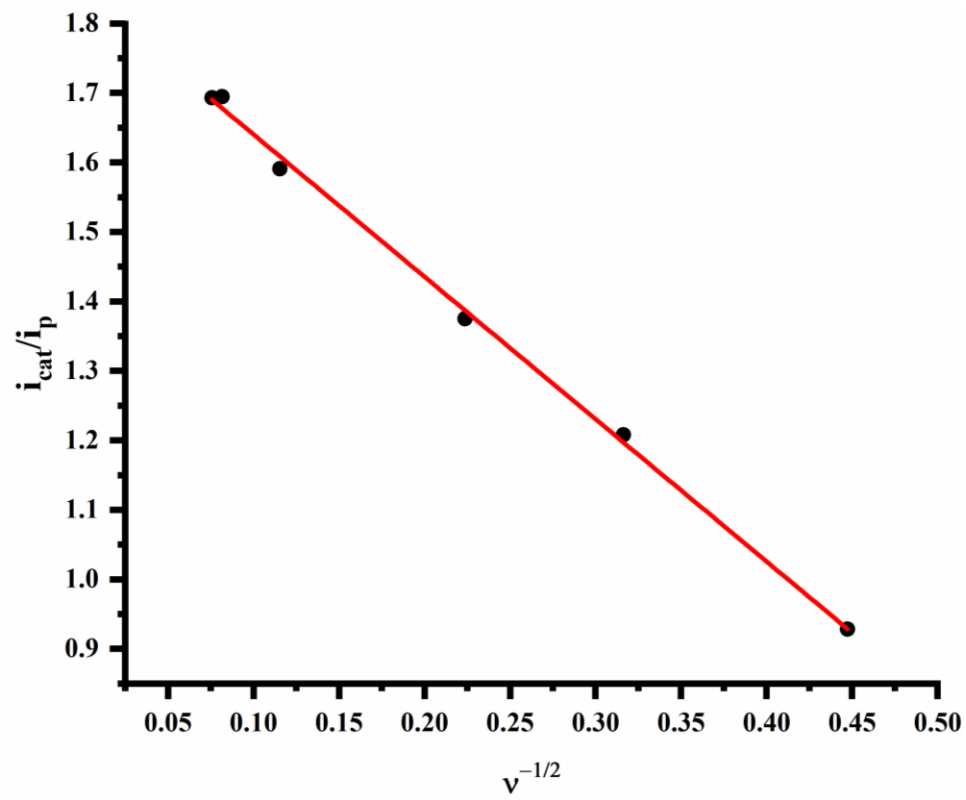

Figure S6. Corresponding linear plot (for OER) of i_{cat}/i_p *vs.* $\nu^{-1/2}$ at different scan rates. %R-square = 99.77.

OER by zinc selenolate complex 1 at different concentrations

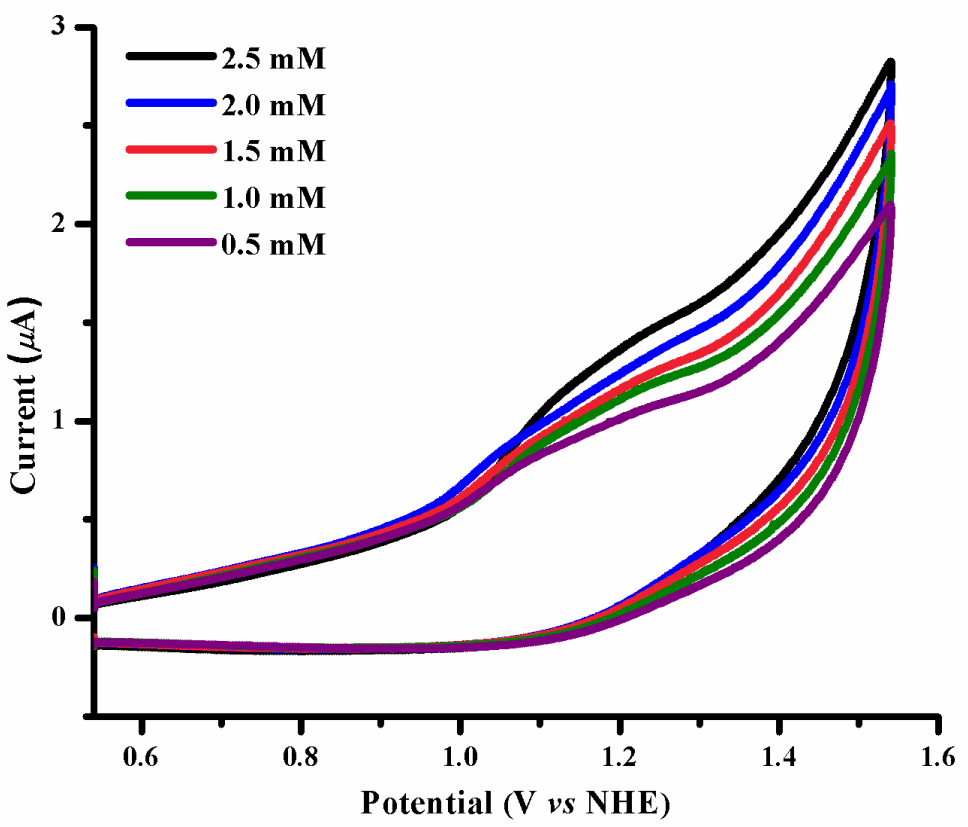

Figure S7 Cyclic Voltammogram of bimetallic zinc selenolate **1** using 0.1M $^{n}Bu_4NPF_6$ as supporting electrolyte in propylene carbonate solution with varying the concentration of catalyst at 20 mV/s

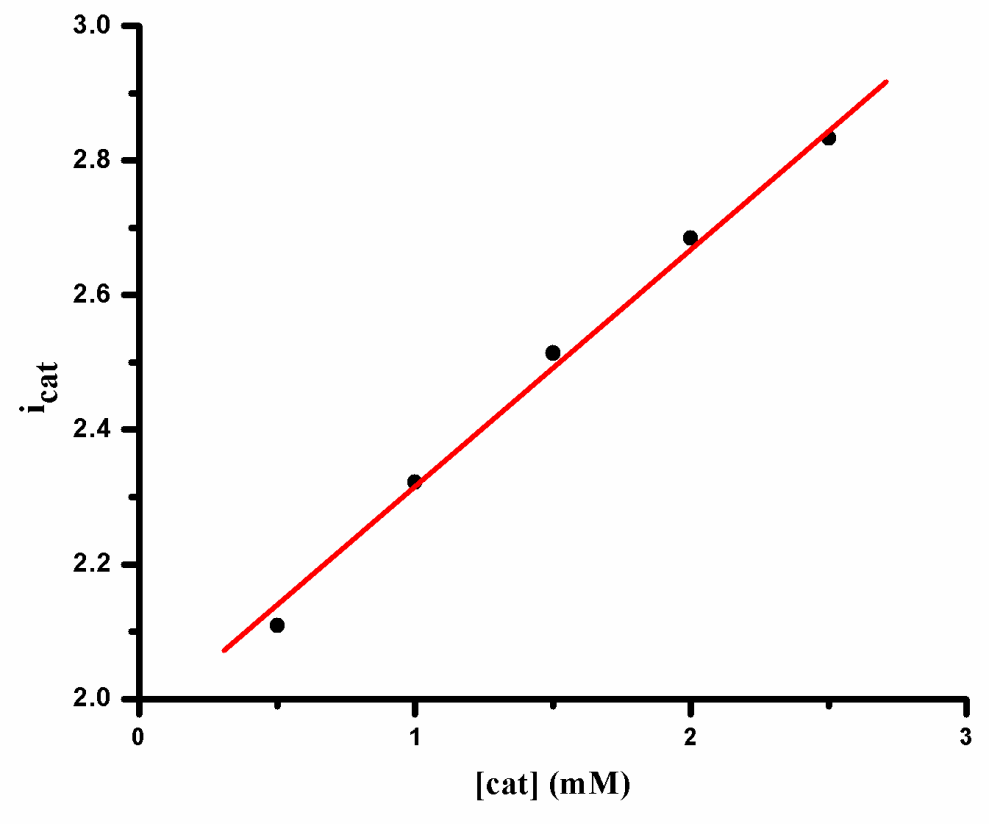

Figure S8. Corresponding linear plot of i_{cat} *vs.* [cat.] in positive direction at 20 mV/s scan rate. %R- square = 99.36.

HER by zinc selenolate complex 1 with water

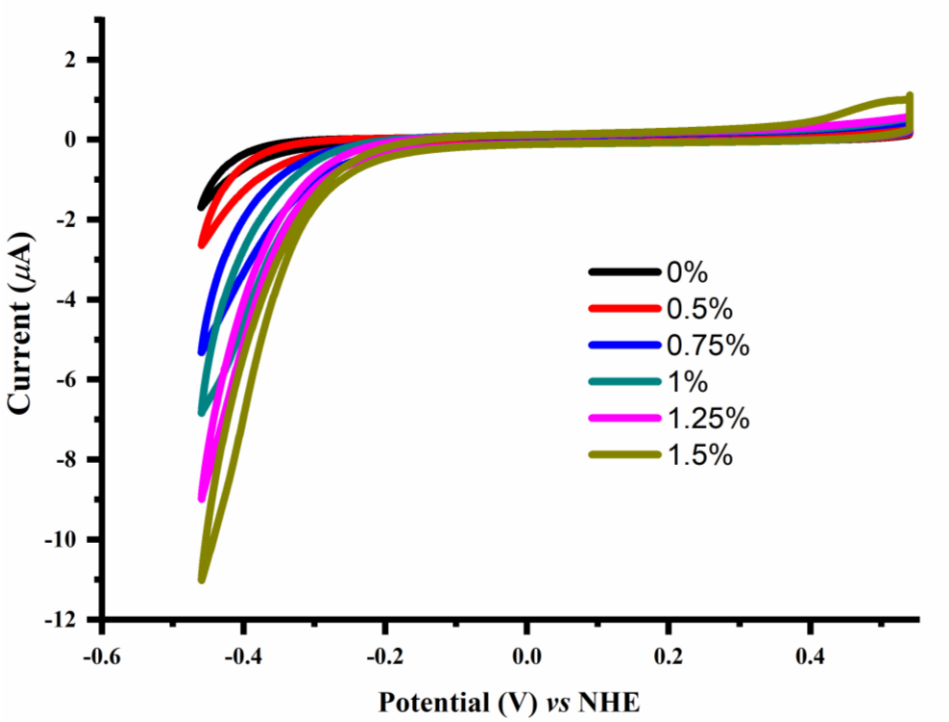

Figure S9. Cyclic Voltammogram of bimetallic zinc selenolate **1** (1mM) using 0.1M $^{n}Bu_4NPF_6$ as supporting electrolyte in propylene carbonate solution with varying the concentration of water up to 1.5% for hydrogen evolution reaction (HER) from water.

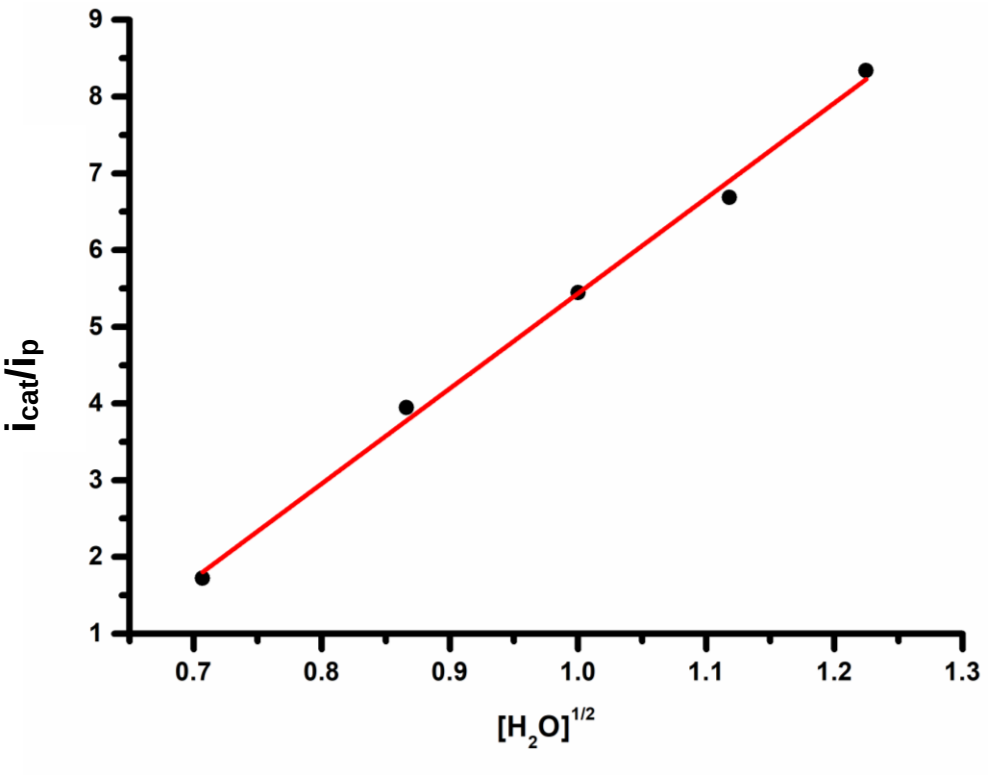

Figure S10. Corresponding linear plot (for HER) of i_{cat} *vs.* $[H_2O]^{1/2}$ with scan rate 20 mV/s.

%R- square = 99.507, slope = 12.406 ± 0.43647

Tafel Plot for hydrogen evolution reaction

TableS1. Tafel plot for hydrogen evolution reaction by zinc selenolate catalyst **1**

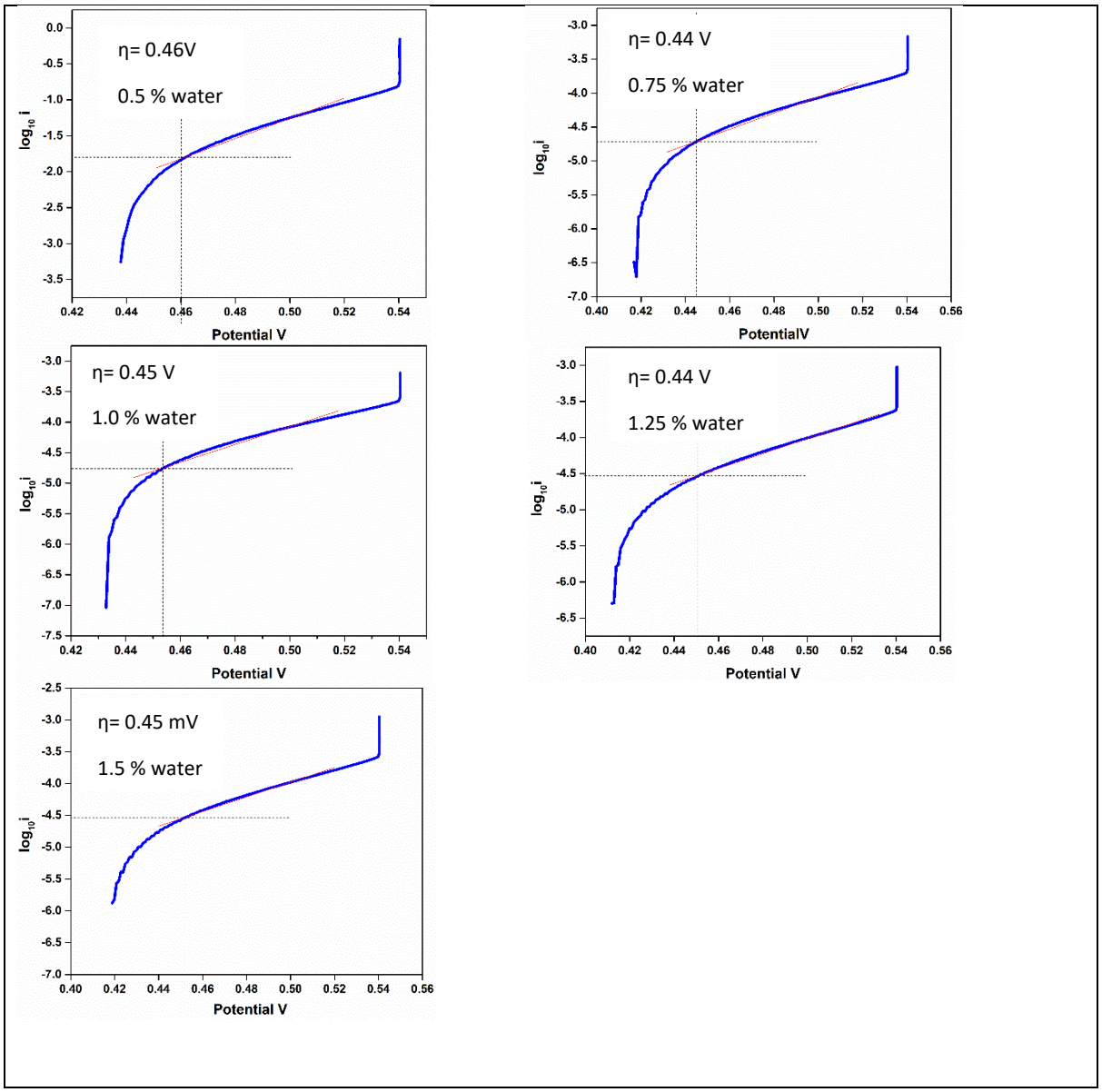

Electrocatalysis of zinc selenolate complex 1 at different scan rates

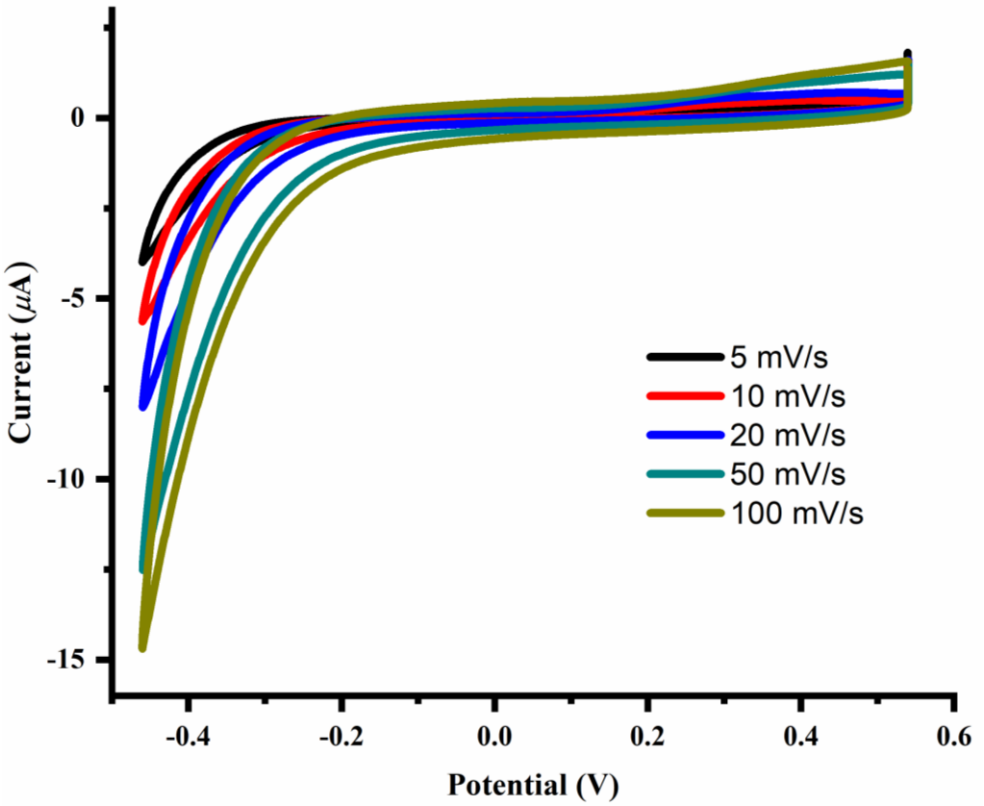

Figure S11 Cyclic Voltammogram of bimetallic zinc selenolate **1** (1mM) using 0.1M $^{n}Bu_4NPF_6$ as supporting electrolyte in propylene carbonate solution with 1% of water at varying scan rates from 5 mV/s to 100 mV/s for hydrogen evolution reaction (HER) from water

HER by zinc selenolate complex 1 at different concentrations

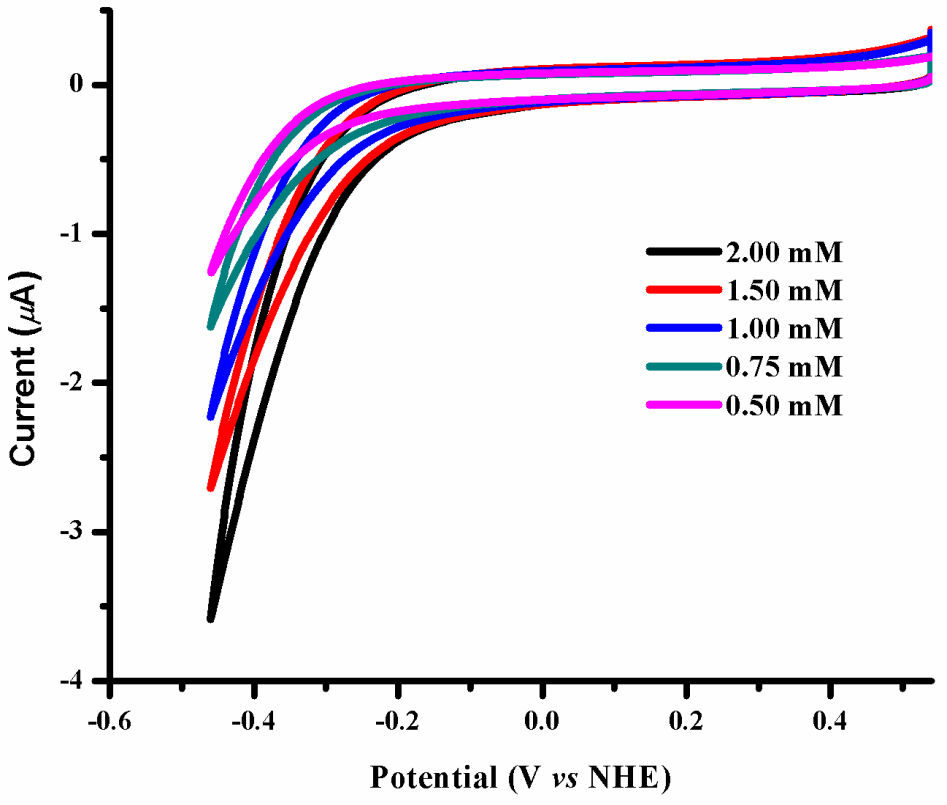

Figure S12 Cyclic Voltammogram of bimetallic zinc selenolate **1** using 0.1M $^{n}Bu_4NPF_6$ as supporting electrolyte in propylene carbonate solution with varying concentration of catalyst at 20 mV/s in cathodic direction.

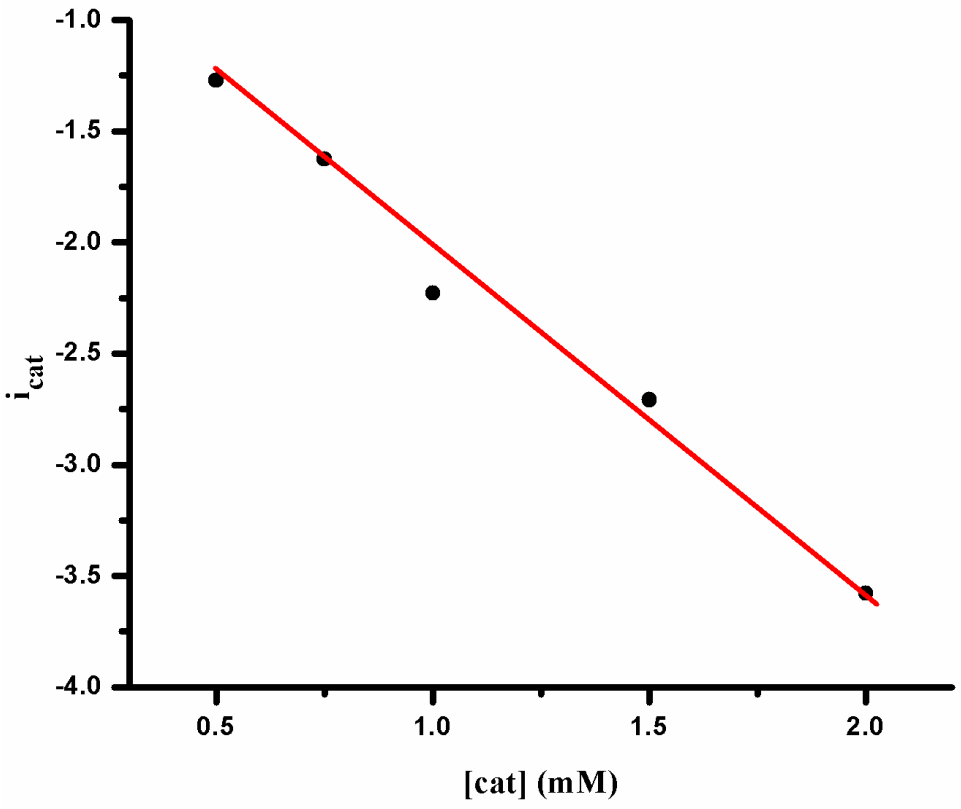

Figure S13. Corresponding linear plot of i_{cat} *vs.* [cat] in cathodic direction at 20mV/s scan rate. %R- square = 98.22.

HER from aqueous acetic acid by zinc selenolate complex 1

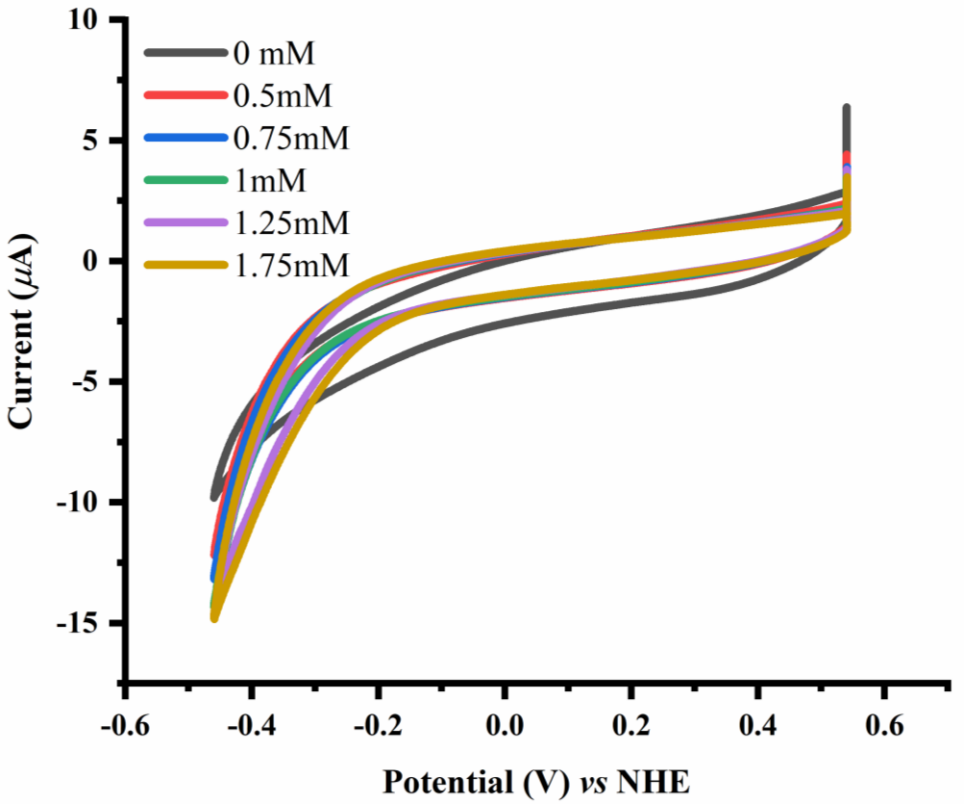

Figure S14. Cyclic Voltammogram of bimetallic zinc selenolate **1** (1mM) using 0.1M $^{n}Bu_4NPF_6$ as supporting electrolyte in propylene carbonate solution with varying the concentration of aqueous acetic acid (AcOH) up to 1.75% for hydrogen evolution reaction (HER).

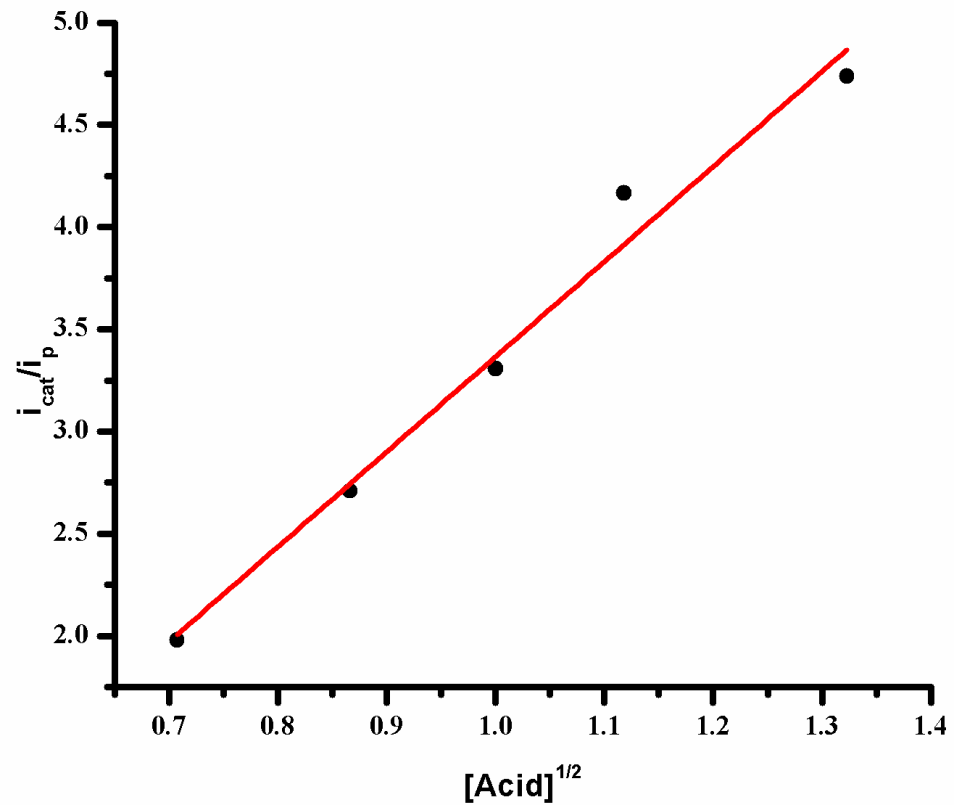

Figure S15. Corresponding linear plot (for HER) of i_{cat} *vs.* [aq. AcOH]$^{1/2}$ with scan rate 20 mV/s. %R- square = 97.65, slope = 4.64 ± 0.3583

HER from aqueous TFA by zinc selenolate complex 1

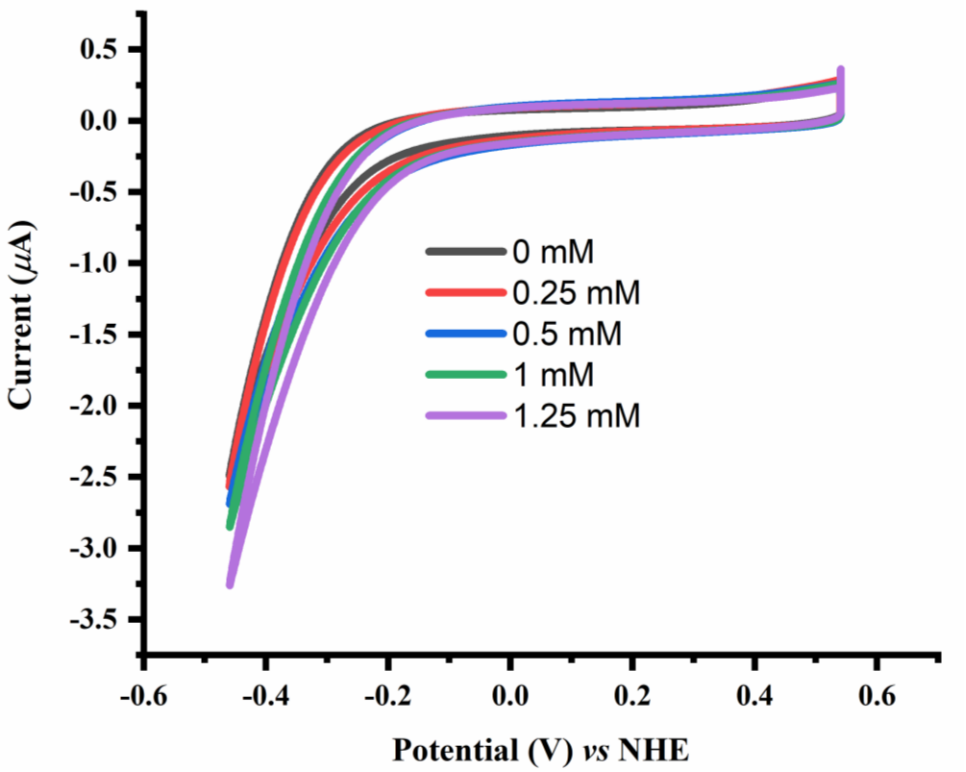

Figure S16. Cyclic Voltammogram of bimetallic zinc selenolate **1**(1mM) using 0.1M $^{n}Bu_4NPF_6$ as supporting electrolyte in propylene carbonate solution with varying the concentration of trifluoroacetic acid (TFA) up to 1.25% for hydrogen evolution reaction (HER).

EDEX and SEM study before CPE

Spectrum processing: Peaks possibly omitted: 0.272, 0.520, 4.150 keV

Processing option: All elements analyzed (Normalized), Number of iterations = 1

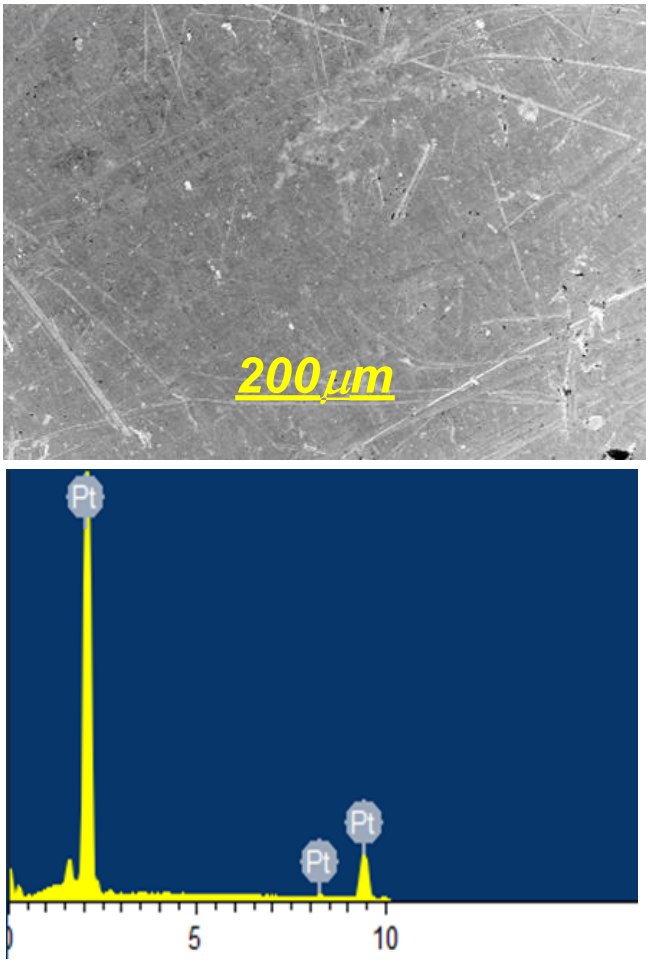

Figure S17. SEM and EDEX images of Pt surface before constant potential electrocatalysis of catalyst **1** using 0.1M $^{n}Bu_4NPF_6$ as supporting electrolyte in propylene carbonate solution.

EDEX and SEM study after CPE

Spectrum processing: Peaks possibly omitted: 0.273, 0.517 keV

Processing option: All elements analyzed (Normalized), Number of iterations = 1

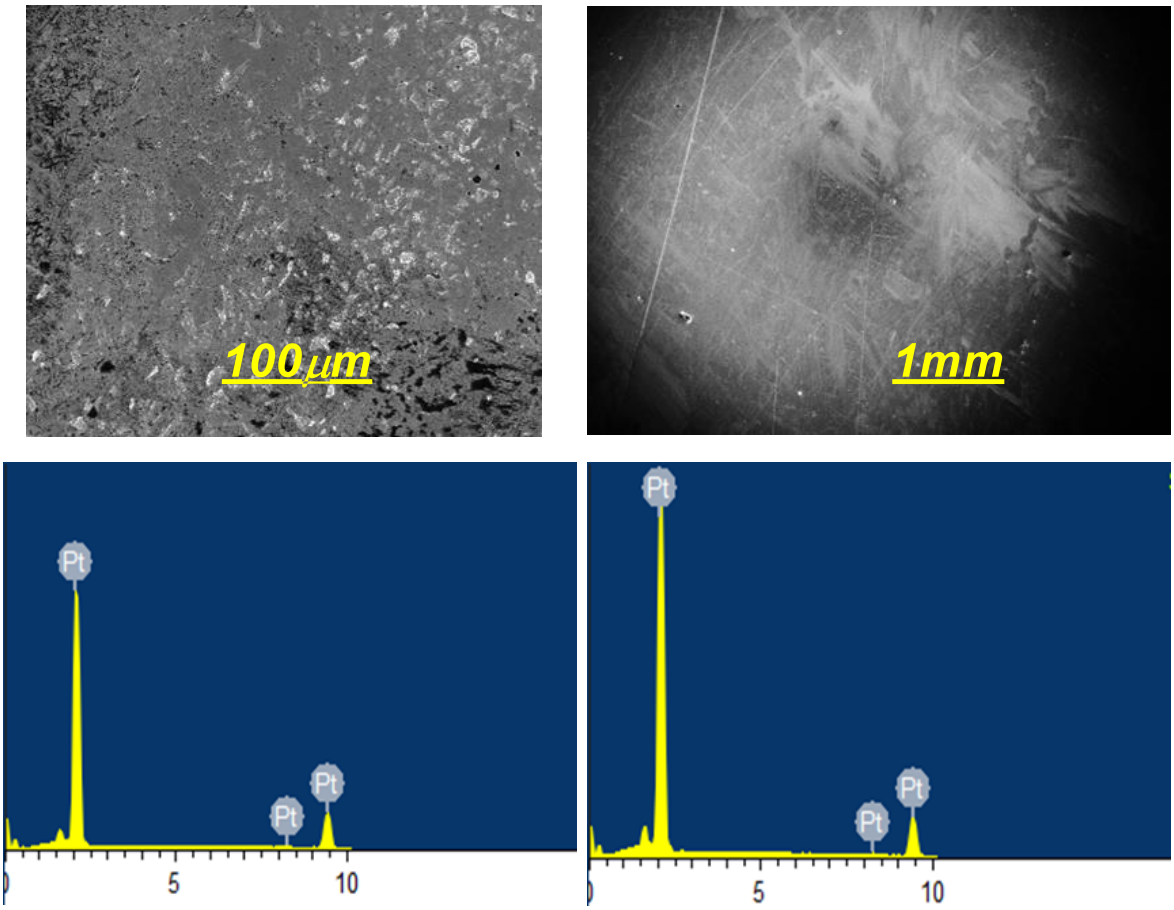

Figure S18. SEM and EDEX images of Pt surface after constant potential electrocatalysis for 2 h of catalyst **1** using 0.1M $^{n}Bu_4NPF_6$ as supporting electrolyte in propylene carbonate solution.

Constant Potential Electrolysis (CPE) of zinc selenolate complex 1 for 2 h in anodic direction for oxygen evolution reaction

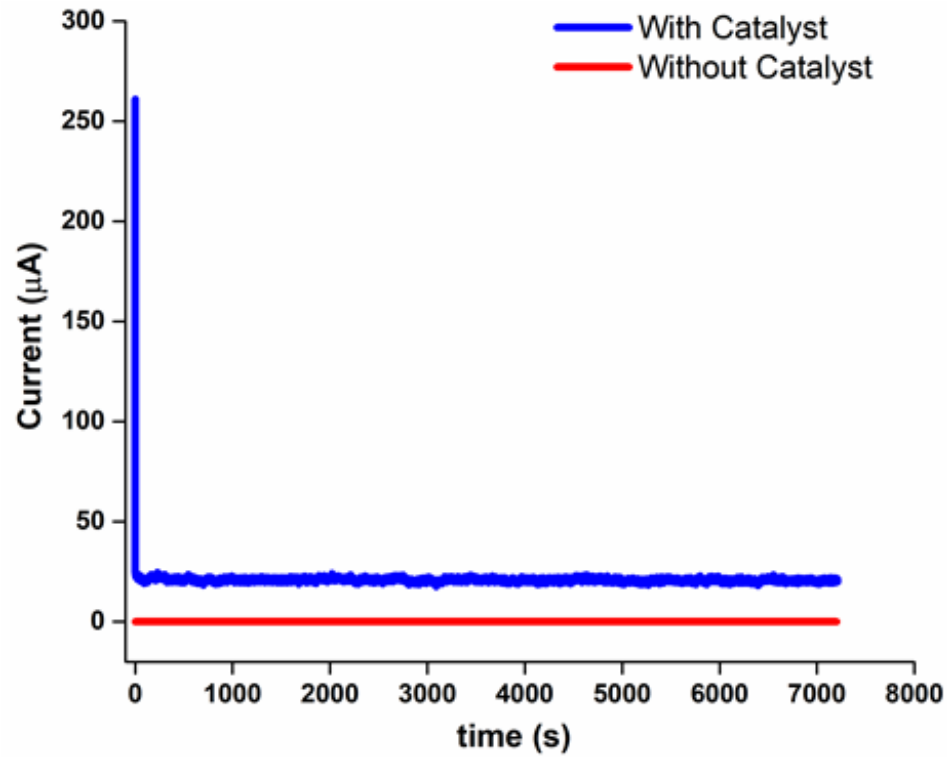

Figure S19. Constant Potential Electrolysis for 2 h at 1.34 V. *vs.* NHE of catalyst **1** (5mM) using 0.1M $^{n}Bu_4NPF_6$ as supporting electrolyte in propylene carbonate solution.

Constant Potential Electrolysis (CPE) of zinc selenolate complex 1 for 2 h in cathodic direction for hydrogen evolution reaction

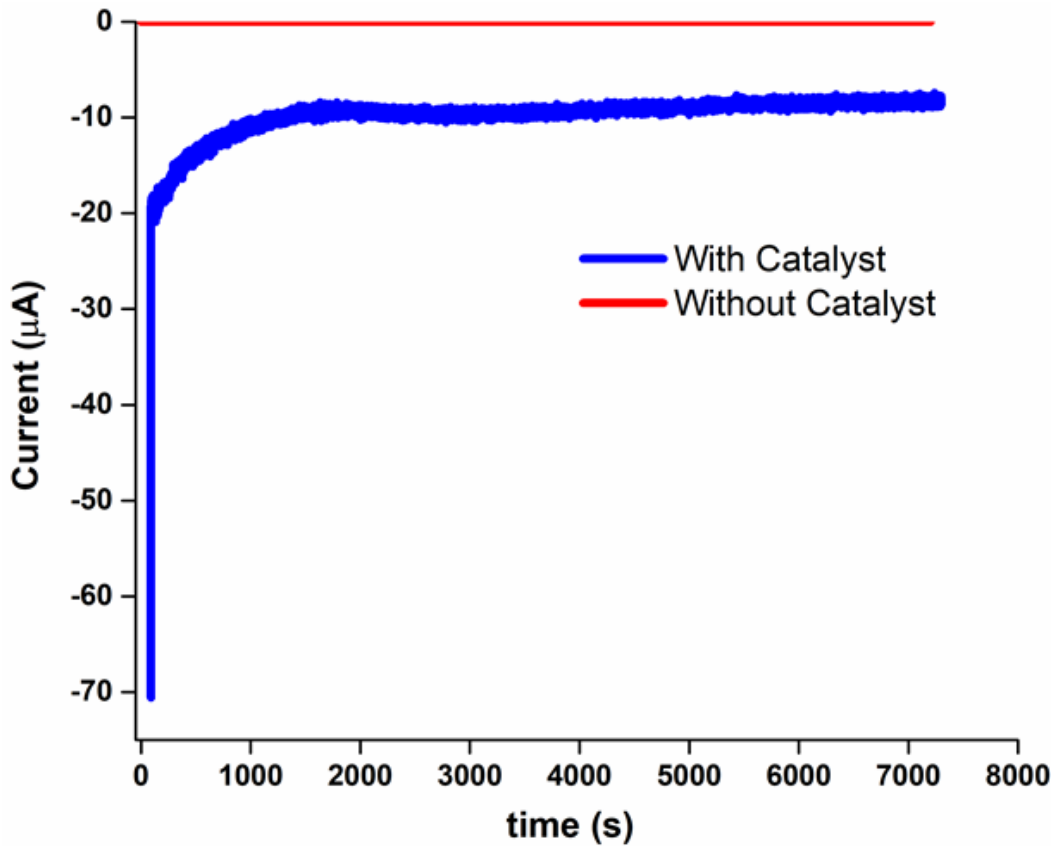

Figure S21. Constant Potential Electrolysis for 2 h at -0.26 V *vs.* NHE for catalyst **1** (5mM) using 0.1M $^{n}Bu_4NPF_6$ as supporting electrolyte in propylene carbonate solution.

UV-vis spectrum after CPE

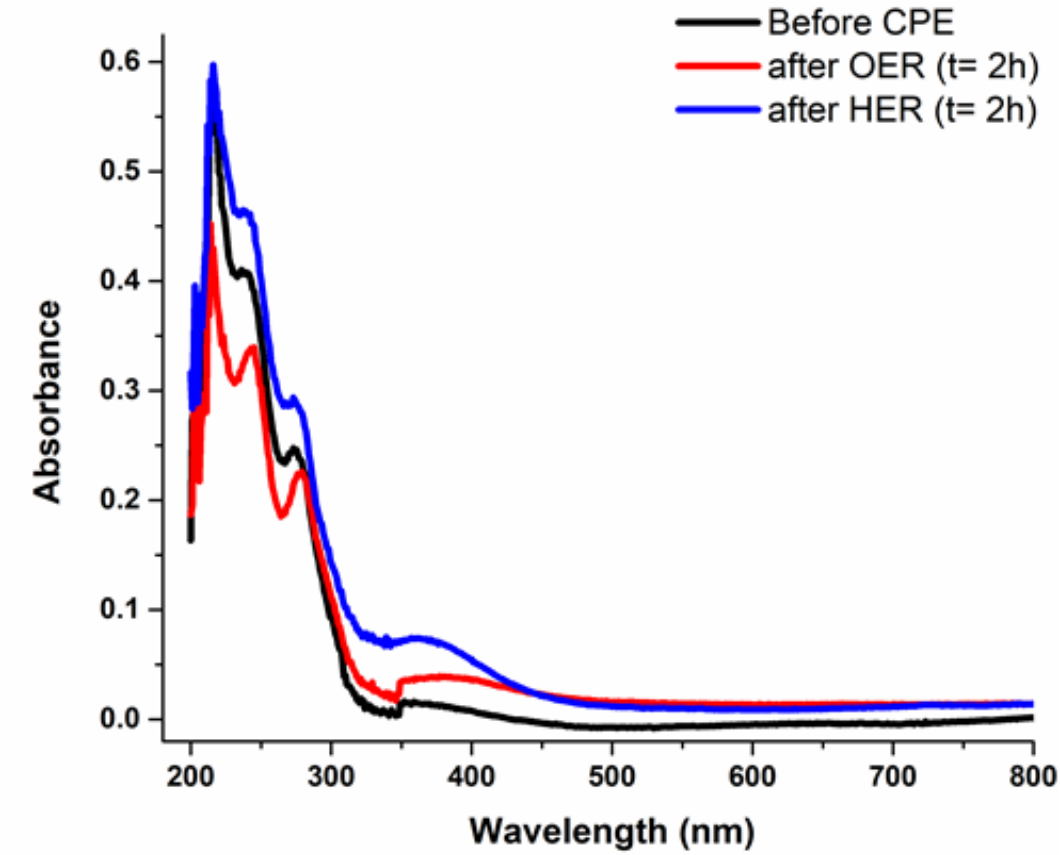

Figure S21. UV-Vis spectrum of zinc catalyst **1** containing electrocatalysis solution before (black) and after the constant potential electrolysis (red and blue) for 2 h.

Oxygen-quantification and Faradic efficiency:

A HI 764080 Digital polarographic dissolved oxygen probe was chosen to measure the change of dissolved oxygen concentration in propylene carbonate solution kept in a four-mouth sealed electrode cell during control potential electrolysis (CPE). The experiments have been carried out by holding the ITO electrode potential at 1.34 V *(vs*. NHE) to 20 min for catalyst **1**. Before performing the chronoamperometry experiment, the sensor was calibrated by using two points against solution and air while reaction solution was purged with Ar gas until the probe sensor showed zero O_2 concentration. The Faradaic efficiency was calculated from the total amount of charge (*Q*, C) passed through the cell and the total amount of the produced oxygen n_{O2} (mol). Faradaic efficiency = $4F*n_{O2}/Q$, wherein F is the Faraday constant, considering that the four electrons are needed to produce one oxygen molecule.

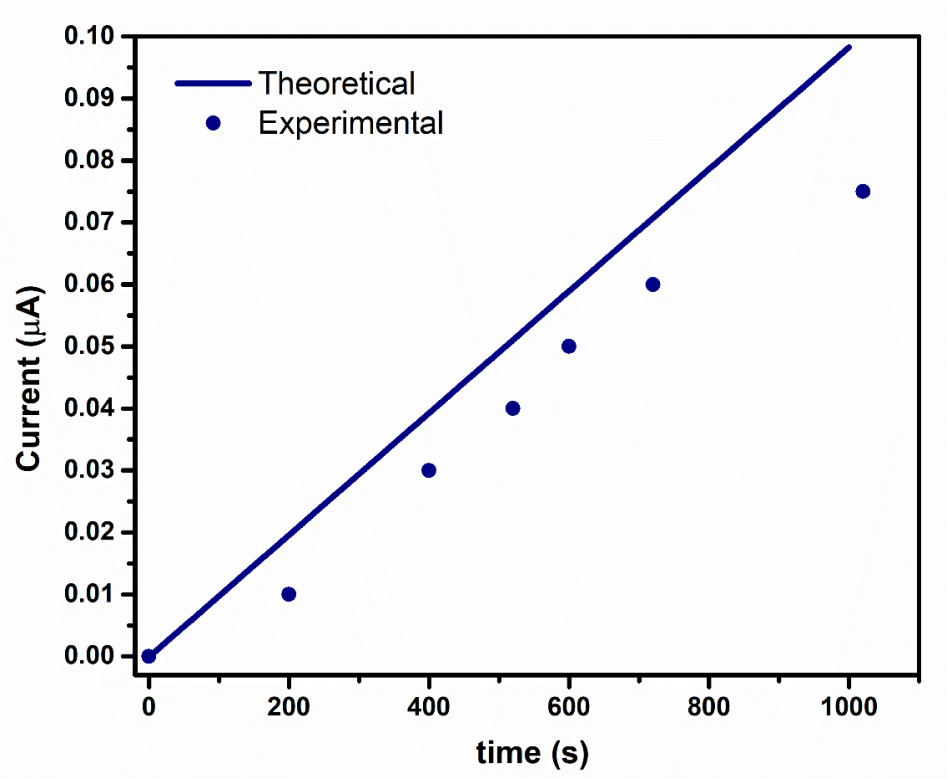

Figure S22. theoretical (blue line) and experimental (blue circle) quantification of O_2 evolution of catalyst **1** at a constant potential of 1.34 V (*vs.* NHE) using ITO working electrode in propylene carbonate solution for water oxidation

OER from water by mercuric selenolate complex 4

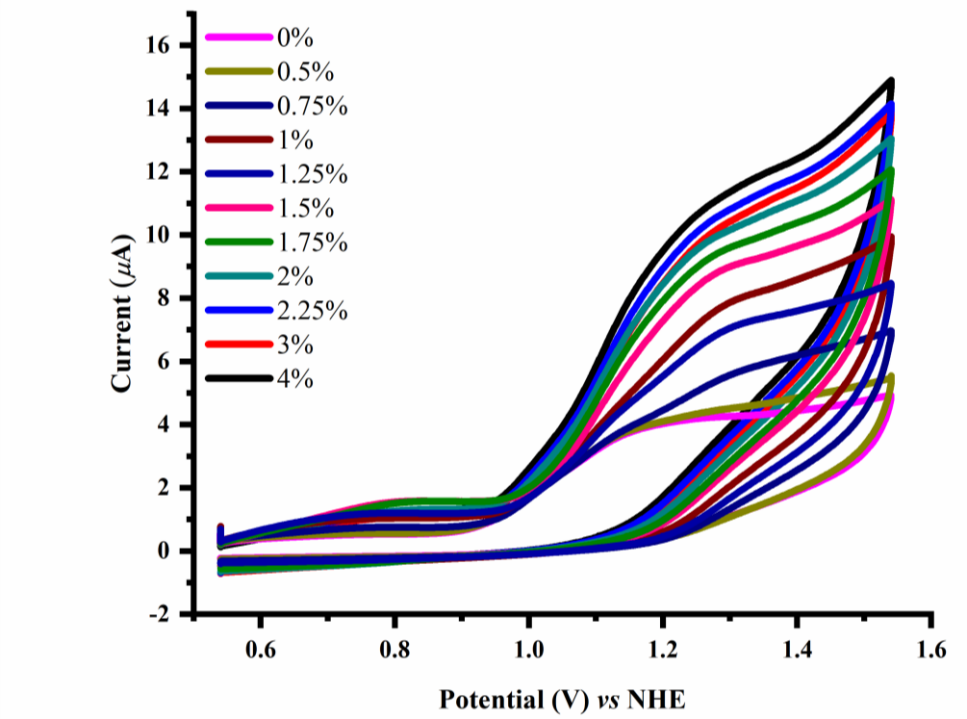

Figure S23. Cyclic Voltammogram of monometallic mercury selenolate **4** (1mM) using 0.1M $^{n}Bu_4NPF_6$ as supporting electrolyte in propylene carbonate solution. with carrying the concentration of water up to 2.0% for oxygen evolution reaction (OER) from water.

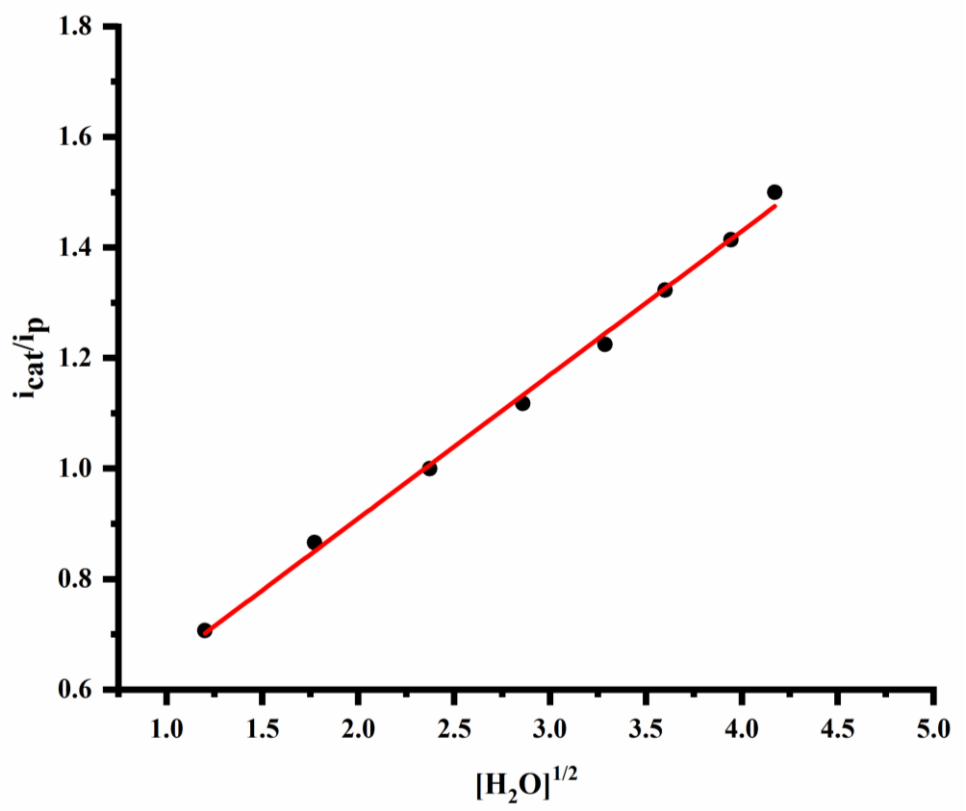

Figure S24. Corresponding linear plot (for OER) of i_{cat} *vs.* $\nu^{-1/2}$ at varying water concentration for mercury selenolate complex **4**. %R- square = 99.70, Slope = 0.259 ± 0.005.

Electrocatalysis at different scan rates

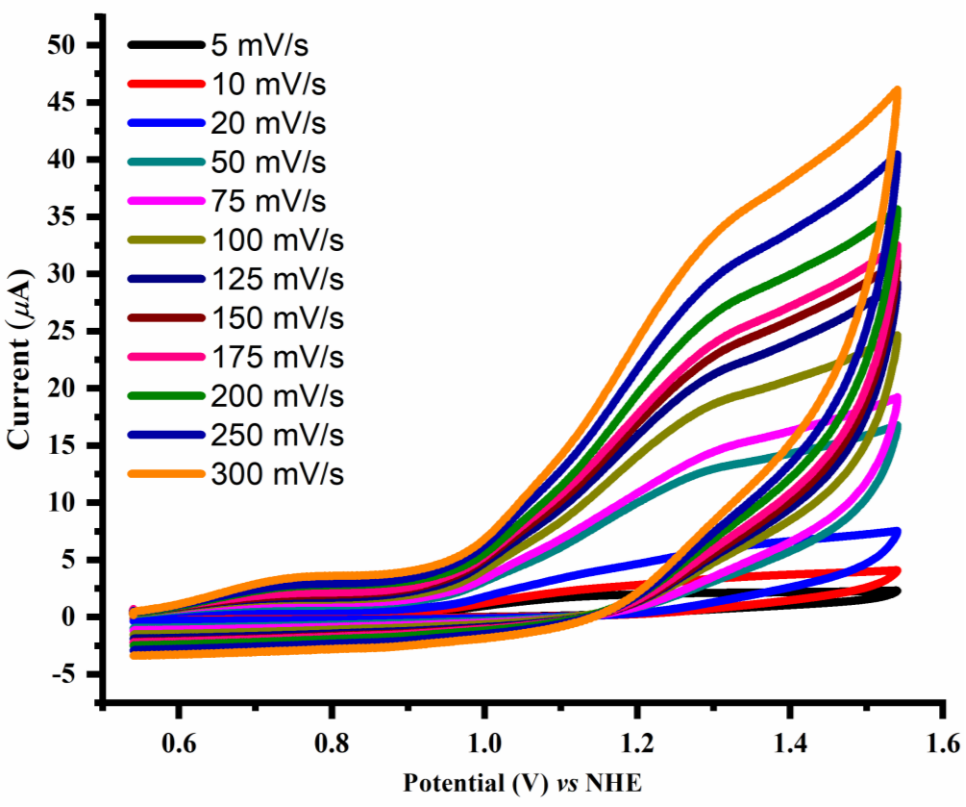

Figure S25 Cyclic Voltammogram of monometallic mercury selenolate **4** (1mM) using 0.1M nBu_4NPF_6 as supporting electrolyte in propylene carbonate solution with carrying the 1% of water at varying scan rates from 5 to 300 mV/s for oxygen evolution reaction (OER) from water.

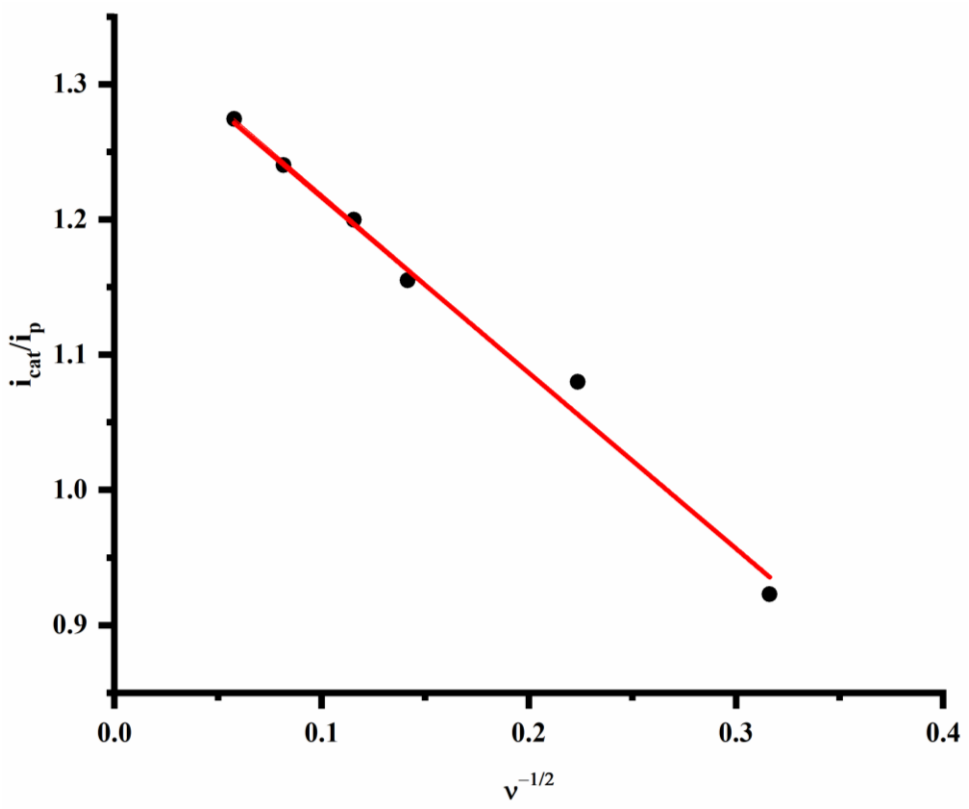

Figure S26. Corresponding linear plot (for OER) of i_{cat} *vs.* $\nu^{-1/2}$ at different scan rates. %R-square = 98.81

HER from water by mercuric selenolate complex 4

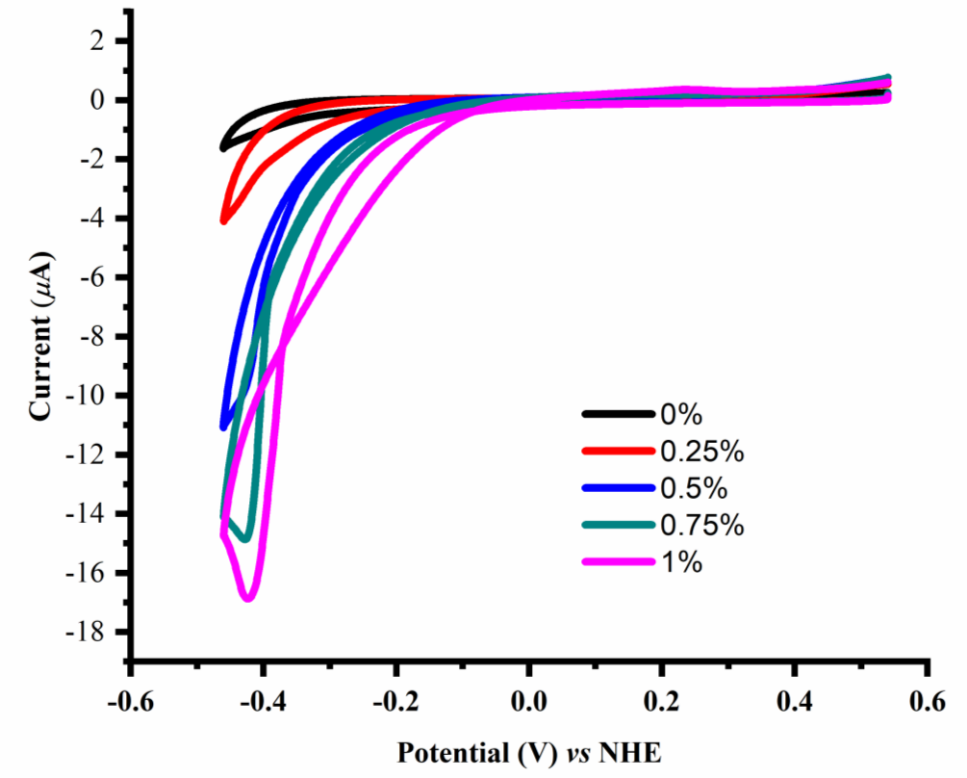

Figure S27. Cyclic Voltammogram of monometallic mercury selenolate **4** (1mM) using 0.1M $^{n}Bu_4NPF_6$ as supporting electrolyte in propylene carbonate solution with carying the concentration of water up to 2.0% for hydrogen evolution reaction (HER) from water

OER from Water by ligand 3

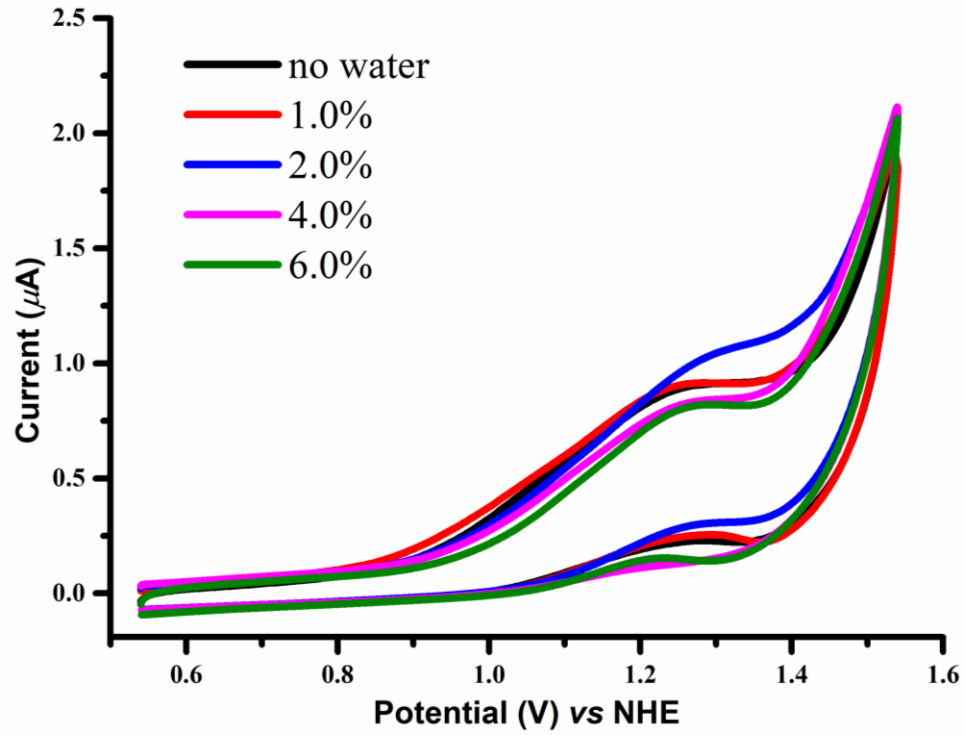

Figure S28. Cyclic Voltammogram of diselenide ligand **3** (1mM) using 0.1M $^{n}Bu_4NPF_6$ as supporting electrolyte in propylene carbonate solution with carying the concentration of water up to 6% for oxygen evolution reaction (OER) from water.

OER from Water by $ZnCl_2$

The CV study of $ZnCl_2$ was done in ethanol due to the insolubility of $ZnCl_2$ in propylene carbonate.

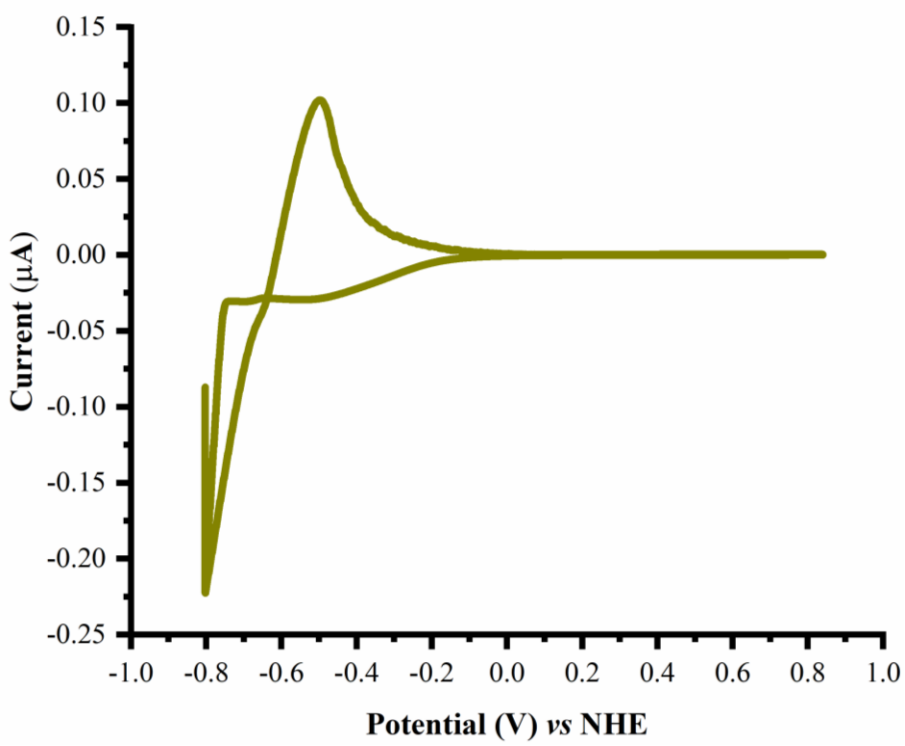

Figure S29. Cyclic Voltammogram of $ZnCl_2$ (2mM) in ethanol solution, which got decomposed after one CV cycle.

Mechanistic Pathways for the Oxygen evolution Reaction

In the zinc selenolate complex **1**, selenium is electronically saturated, valency wise divalent, and hence poor electrophile. However, it could be a better 2 electron donor. Here in the following reaction scheme, the nucleophilic character of selenium in the ligand core of zinc selenolate complex **1** have been shown.

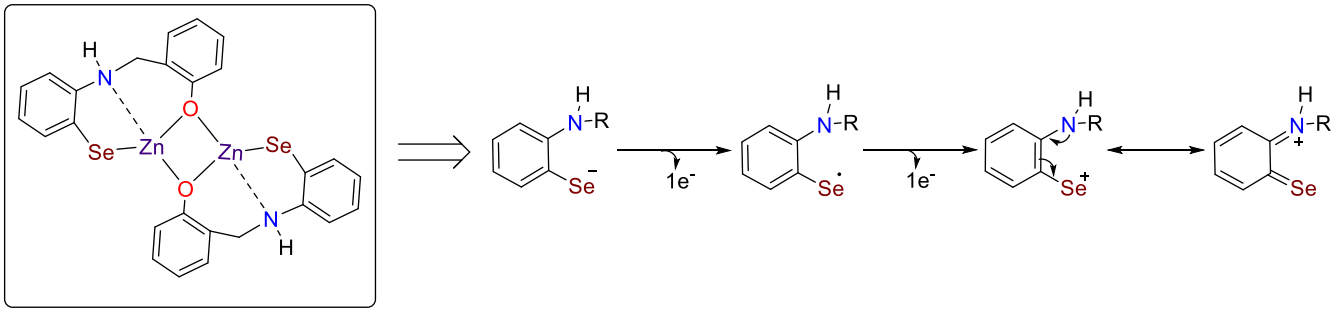

The favorable pathway for the oxygen evolution from electrocatalytic water splitting on the basis of change in Gibb's free energy. The potential determining step is the fourth proton coupled electron transfer (PCET) step i.e. the formation of species **1e** for which the calculated ΔG is 62.64 kcalmol^{-1}. The calculated overpotential for the PDS is 1.49 V.

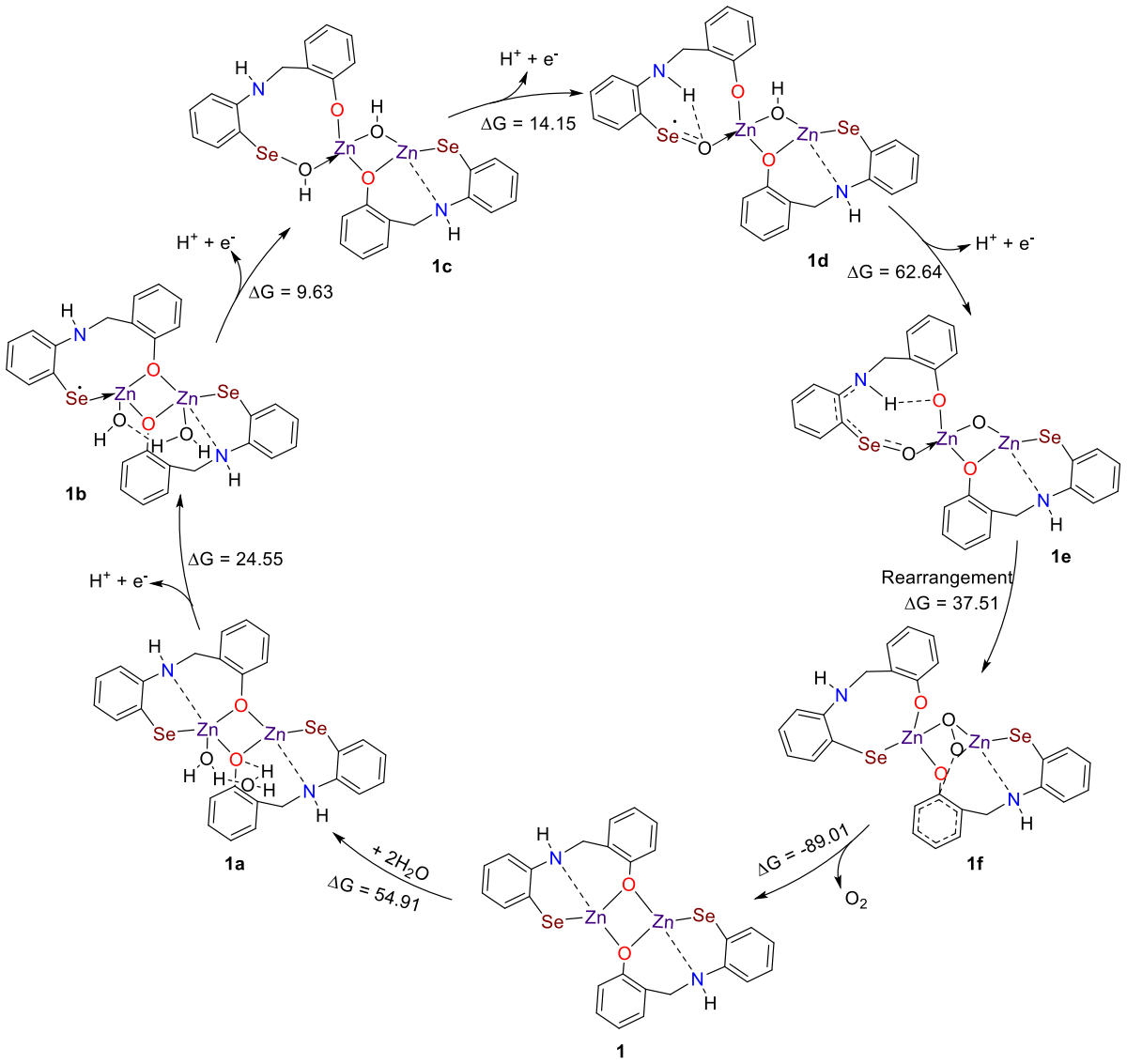

Scheme S2. Elaborated proposed mechanism for OER by catalyst **1** of Scheme 3. The free energy (in kcal mol^{-1}) have been calculated in B3LYP/def2-TZVP level of theory.

Mechanistic Pathways for the Hydrogen evolution Reaction

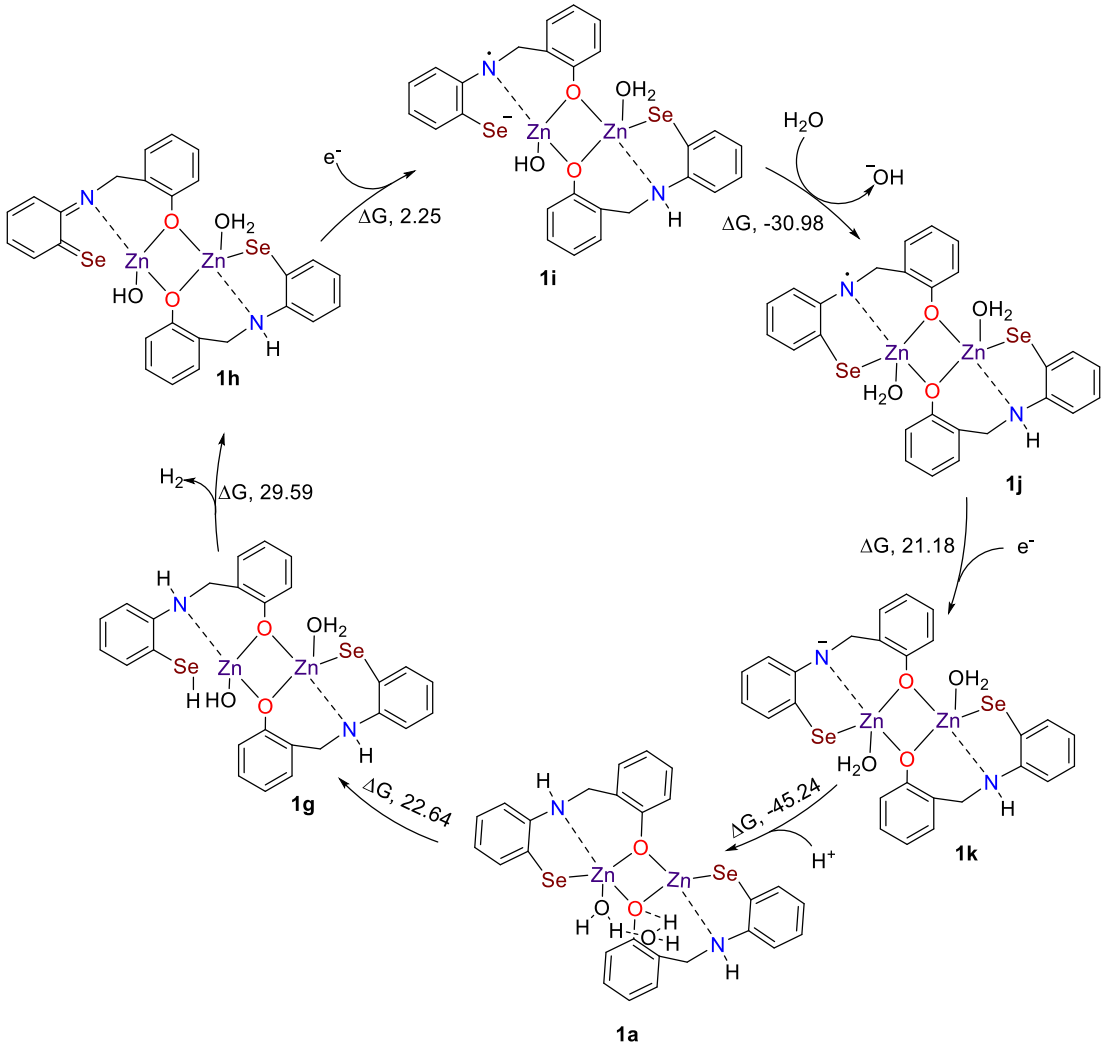

Scheme S3. Elaborated proposed mechanism for HER by zinc selenolate **1** of Scheme 3. The free energy (in kcal mol^{-1}) have been calculated in B3LYP/def2-TZVP level of theory.

Computational Methods

All the electronic structure calculations presented in this work were performed using density functional theory implemented in TURBOMOLE 7.4[3] electronic structure package. Optimization of molecular geometry in gas phase were carried out using B3LYP[4-6] hybrid functional. The electronic configuration of the atoms was described with def2-TZVP[7] basis set. For all the calculations resolution of identity (RI) approximation with corresponding auxiliary basis set was used to speed up the calculations. Stability of the optimized geometries were confirmed by absence of imaginary vibrational frequencies. Thermal corrections to Gibbs free energy including zero-point energy were obtained from vibrational frequency analysis at same level of theory at 298.15 K and 1 atm within ideal-gas rigid-rotor harmonic-oscillator approximations.

In case of OER, proton and electron transfer steps are considered as proton-coupled electron transfer (PCET) steps. In standard hydrogen condition, proton and electron are in equilibrium with hydrogen ($H^+ + e^- \rightleftharpoons ½\ H_2$). Therefore, the Gibbs free energy of proton coupled electron can be written as half of free energy of hydrogen molecule.

In case of HER, individual proton and electron transfers cannot be modeled as PCET. Instead, the chemical potential of proton (μ_{H+}) and electron (μ_e) are calculated as follows[8]:

$$\mu_{H+}(pH) = \mu_{H+}(pH=0) – 2.3RT\ pH$$

where $\mu_{H+}(pH=0)$ was taken as G_{H+} (=H -TS) in the gas phase at 1atm plus hydration energy[9] (264 kcal/mol) at 1 M. The chemical potential of a proton is calculated at neutral condition (pH=7).

$$\mu_e(E) = \mu_e(SHE) – e.E$$

where μ_e(SHE) was taken as G_e which is calculated as difference of half of Gibbs free energy of hydrogen and Gibbs free energy of proton under SHE condition. E and e represent electron potential of HER (0.425 V) and electronic charge, respectively.

The mechanisms of OER (path-A and path-B) and HER are depicted in Scheme S2 – S3 and corresponding reaction Gibbs free energies are presented in Table S3–S4.

The electronic structure analysis of along OER pathway is presented in Figure S30. The number of electrons changes by one in every PCET step. For the intermediate with odd number of electrons the spin density (SD) is plotted to determine the localization of unpaired electron. In **1a** HOMO is located on Se, phenyl ring and N. Therefore, the electron removal in the PCET step will be from this region. The SD of unpaired electron in **1b** is also on the same Se, ring and N. This indicates that Se undergoes oxidation (Se^{2-} to Se^{-1}) during this PCET step. It is also confirmed by natural bond order (NBO) analysis that electronic charge on Se and N decrease from 0.43 e and 0.70 e in **1a** to 0.14 e and 0.44 e in **1b**, respectively. Here charges on Se and N are in equilibrium with phyneyl ring. As also evidenced in further steps, Se seems to play important role in OER reaction.

Table S2. Comparison of bond lengths and bond angles of experimentally obtained structure of bimetallic zinc selenolate complex **1** (see Table S2) and calculated structure using DFT/B3LYP/def2-TZVP. In experiment, bimetallic zinc selenolate complex **1** crystallizes with dimethyl sulfoxide (DMSO) coordinated to Zn. In DFT calculations the bimetallic zinc selenolate complex **1** molecule is considered with adsorption of 1) water and 2) DMSO. Relative error presented here are calculated as ((calculated – experimental)/ experimental)*100.

Relative error percentage in bond lengths		
Bond	**Calculated with DMSO adsorbed**	**Calculated with H_2O adsorbed**
Se1—C1	1.05	1.05
Se1—Zn1	0.18	-2.68
Zn1—O1	0.44	-0.54
Zn1-N1	4.14	-1.77
Zn1—O1^{1}	1.55	-4.76

Relative error percentage in bond angles		
Bond Angles	**Calculated with DMSO adsorbed**	**Calculated with H_2O adsorbed**
C1-Se1-Zn1	3.14	1.86
Se1-Zn1-N1	-0.02	11.37
Zn1-N1-C6	2.02	2.59
O1-Zn1-O1^{i}	2.81	3.70
Zn1^{1}-O1-Zn1	-2.16	-2.33

Table S3. Reaction free energies of OER on the catalyst **1**.

Reaction Step		**ΔG (eV)**	**ΔG (kcal/mol)**
1	**1** + $2H_2O$ → **1a**	2.38	54.91
2	**1a** → **1b** + ($H^+ + e^-$)	1.06	24.55
3	**1b** → **1c** + ($H^+ + e^-$)	0.42	9.63
4	**1c** → **1d** + ($H^+ + e^-$)	0.61	14.15
5	**1d** → **1e** + ($H^+ + e^-$)	2.72	62.64
6	**1e** → **1f**	1.63	37.51
7	**1f** → **1** + O_2	-3.86	-89.01

Table S4. Reaction free energies of HER on the catalyst **1**.

	Reaction Step	ΔG (eV)	ΔG (kcal/mol)
1	**1a** → **1g**	0.98	22.64
2	**1g** → **1h** + H_2	1.28	29.59
3	**1h** + e^- → **1i**	0.097	2.25
4	**1i** + H_2O → **1j** + OH^-	-1.37	-30.98
5	**1j** + e^- → **1k**	0.91	21.18
6	**1k** + H^+ → **1a**	-1.96	-45.24

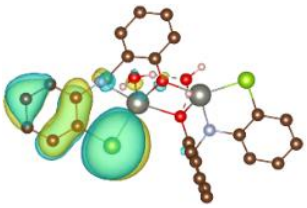

1a, HOMO

(Even e^-s)

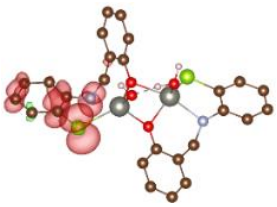

1b, SD

(Odd e^-s)

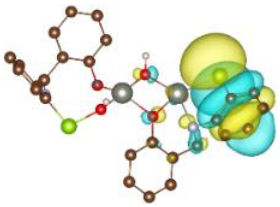

1c, HOMO

(Even e^-s)

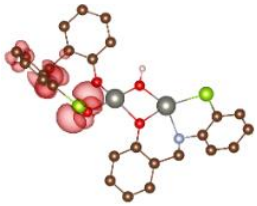

1d, SD

(Odd e^-s)

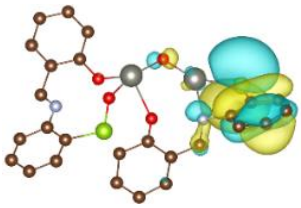

1e, HOMO

(Even e^-s)

Figure S30 Electronic structure analysis of OER path-A. HOMOs and spin densities (SDs) are plotted at isosurface value of 0.02 and 0.003 a_0^{-3}, respectively. Red and green SDs represent up and down spin electrons. SDs are plotted only for the intermediates that have odd number of electrons. For the convenience, H of adsorbate only are shown here.

References

1 Pavlishchuk, V. V. & Addison, A. W. Conversion constants for redox potentials measured versus different reference electrodes in acetonitrile solutions at 25°C *Inorg. Chim. Acta* ***298***, 97–102 (**2000)**.

2 Balkrishna, S. J., Bhakuni, B. S. & Kumar, S. Copper catalyzed/mediated synthetic methodology for ebselen and related isoselenazolones. *Tetrahedron* **67**, 9565–9575 (2011).

3 Rathore, V., Upadhyay, A. & Kumar, S. A organodiselenide with dual mimic function of sulfhydryl oxidases and glutathione peroxidases: aerial oxidation of organothiols to organodisulfides. *Org. Lett.* **20**, 6274–6278 (2018).

4 Furche, F., Ahlrichs, R., Hättig, C., Klopper, W., Sierka, M. & Weigend, F. Turbomole. *WIREs Comput. Mol. Sci.* **4**, 91–100 (2014).

5 Becke, A. D. Density-functional exchange-energy approximation with correct asymptotic behaviour. *Phys. Rev. A* **38**, 3098–3100 (1988).

6 Lee, C., Yang, W. & Parr, R. G. Development of the Colle-Salvetti correlation-energy formula into a functional of the electron density. *Phys. Rev. B* **37**, 785–789 (1988).

7 Becke, A. D. Density-functional thermochemistry. III. The role of exact exchange. *J. Chem. Phys.* **98**, 5648–5652 (1993).

8 Weigend, F. & Ahlrichs, R. Balanced basis sets of split valence, triple zeta valence and quadruple zeta valence quality for H to Rn: Design and assessment of accuracy. *Phys. Chem. Chem. Phys.* **7**, 3297–3305 (2005).

9 Huang, Y., Nielsen, R. J., Goddard, W. A. & Soriaga, M. P. The Reaction Mechanism with Free Energy Barriers for Electrochemical Dihydrogen Evolution on MoS_2. *J. Am. Chem. Soc.* **137**, 6692−6698 (2015).